Final Report: SERDP SI-1260

Detection and Identification of Archaeological Sites and Features Using Radar Data

Submitted by

Co-Principal Investigators:

Dr. Ronald G. Blom, Jet Propulsion Lab, NASA

Dr. Douglas C. Comer, Cultural Site Research and Management, Inc.

REPORT DOCUMENTATION PAGE

Form Approved
OMB No. 0704-0188

1. REPORT DATE *(DD-MM-YYYY)*	2. REPORT TYPE	3. DATES COVERED *(From - To)*
04/26/06	SERDP Project Final Report	2002-2006

4. TITLE AND SUBTITLE
Final Report SERDP CS-1260
Detection and Identification of Archaeological Sites and Features Using Synthetic Aperture Radar (SAR) Dada Collected from Airborne Platforms

5a. CONTRACT NUMBER
1246527

5b. GRANT NUMBER
N/A

5c. PROGRAM ELEMENT NUMBER
N/A

6. AUTHOR(S)
Ronald G. Blom, Ph.D.
Douglas C. Comer, Ph.D.

5d. PROJECT NUMBER
CS-1260

5e. TASK NUMBER
NMO 715477

5f. WORK UNIT NUMBER
Task Plan 82-6578

7. PERFORMING ORGANIZATION NAME(S) AND ADDRESS(ES)
JPL/NASA, 4800 Oak Grove Drive, Pasadena, CA 91109
Cultural Site Research and Management, 4303 N. Charles St. Baltimore, MD 21218

8. PERFORMING ORGANIZATION REPORT NUMBER
N/A

9. SPONSORING/MONITORING AGENCY NAME(S) AND ADDRESS(ES)
SERDP Program Office
901 North Stuart Street, STE 303
Arlington, VA 22203

10. SPONSOR/MONITOR'S ACRONYM(S)
SERDP

11. SPONSOR/MONITOR'S REPORT NUMBER(S)
TBA

12. DISTRIBUTION/AVAILABILITY STATEMENT
Unclassified/unlimited

13. SUPPLEMENTARY NOTES

14. ABSTRACT

The goal of this project was to develop protocols incorporating remote sensing data to significantly increase efficiency in Phase A archaeological surveys of DoE and DoD lands. Our principal, but not exclusive, focus has been on the use of high resolution airborne radar data in detection, inventory, and evaluation of archaeological sites. Principal radar data are from the JPL/NASA AIRSAR which provided multi-band, multi-polarizaiton synthetic aperture radar (SA) data and high resolution DEMs. Improved processing and orthorectification have allowed us for the first time to completely utilized the full capabilities for archaeological applications. The data are used in predicting the distribution of archaeological sites. We developed a predictive model which will enable much more efficient archaeological evaluations, and protocols that will enable incorporation of remote sensing data into more conventional archaeological surveys.

15. SUBJECT TERMS
archaeology, remote sensing, radar, GIS

16. SECURITY CLASSIFICATION OF:			17. LIMITATION OF ABSTRACT	18. NUMBER OF PAGES	19a. NAME OF RESPONSIBLE PERSON
a. REPORT	b. ABSTRACT	c. THIS PAGE			19b. TELEPHONE NUMBER *(Include area code)*
U	U	U	UU	50	

Reset

TABLE OF CONTENTS

LIST OF TABLES

LIST OF FIGURES

ACRONYMS

AIRSAR	Airborne Synthetic Aperture Radar system
C-Band	Standard term for radar bands operating on a wavelength of 7.5 cm - 3.75 cm and a frequency of 4 - 8 GHz
CHH	C-band transmitted in and received in horizontal polarization
CHV	C-band transmitted in horizontal polarization and received in vertical polarization
CVV	C-band transmitted in and received in vertical polarization
CSRM	Cultural Site Research and Management
DEM	Digital Elevation Model
DGPS	Differential processing Geographical Positioning System
DoD	Department of Defense
DTM	Digital Terrain Model
GeoSAR	Geographic Synthetic Aperture Radar
GIS	Geographic Information System
GCP	Ground Control Point
HH	Radar waves transmitted in and received in horizontal polarization
HV	Radar waves transmitted in horizontal polarization and received in vertical polarization
IKONOS	Private sector satellite that acquires multispectral data in these wavelengths and frequencies

Band	Color	Wavelength	Resolution	Resampled Resolution
1	Blue	445-516	4m	1m
2	Green	506-595	4m	1m
3	Red	632-698	4m	1m
4	Near Infrared	757-853	4m	1m
5	Pan	445-853	1m	

JPL Jet Propulsion Laboratory

LANDSAT US Satellite used to acquire remotely sensed data in these wavelengths and resolutions:

Band	Wavelength	Resolution
1 VIS	0.45-0.52	30 m
2 VIS	0.53-0.61	30 m
3 VNIR	0.63-0.69	30 m
4 VNIR	0.78-0.90	30 m
5 SWIR	1.55-1.75	30 m
6 TIR	10.4-12.5	60 m
7 SWIR	2.09-2.35	30 m
8 PAN	0.52-0.90	15 m

L-Band Standard term for radar bands operating on a wavelength of 30 cm - 15 cm and a frequency of 1 - 2 GHz

LHH L-band transmitted in and received in horizontal polarization

LHV L-band transmitted in horizontal polarization and received in vertical polarization

LVV L-band transmitted in and received in vertical polarization

NASA National Aeronautics and Space Administration

NCPTT National Center for Technology Transfer and Preservation

NDVI Normalized Difference Vegetative Index

NSF National Science Foundation

P-Band Standard term for radar bands operating on a wavelength of about 1.3 to 0.3 m and a frequency of 230-1000 MHz

PHH P-band transmitted in and received in horizontal polarization

PVH P-band transmitted in vertical polarization and received in horizontal polarization

PVV P-band transmitted in and received in vertical polarization

SAR Synthetic Aperture Radar

SRTM Shuttle Radar Topography Mission

UCLA	University of California, Los Angeles
VH	Radar waves transmitted in vertical polarization and received in horizontal polarization
VV	Radar waves transmitted in and received in vertical polarization
X-band	standard term for radar bands operating on a wavelength of 2.5-4 cm and a frequency of 8-12 GHz
XVV	X-band transmitted and received in vertical polarization

ACKNOWLEDGEMENTS

Mr. Michael Abrams, NASA Jet Propulsion Laboratory/California Institute of Technology

Mark E. Brender Vice President Communications & Marketing, GeoEye

California State Archaeological Archives, University of California, Fullerton

Dr. Bruce Chapman, NASA Jet Propulsion Laboratory/California Institute of Technology

Dr. Elaine Chapin, NASA Jet Propulsion Laboratory/California Institute of Technology

John Cook, President, ASM, Associates

Dr. Robert Crippen, NASA Jet Propulsion Laboratory/California Institute of Technology

Earth Data Corporation

Mr. Bradley Smith, Executive Director, SERDP

Dr. Robert Holst, Program Manager, SERDP

Katharine Kerr, SERDP Support Office (HydroGeoLogic, Inc.)

Mahta Moghaddam, Associate Professor, Department of Electrical Engineering and Computer Science, University of Michigan.

National Archives and Records Administration (NARA), College Park, Maryland

Space Imaging Corporation

Stacey Otte, Executive Director, Catalina Island Museum, Catalina Island Conservancy

Dr. Mark Raab, University of Missouri-Kansas City.

Eileen Regan, SERDP Support Office (HydroGeoLogic, Inc.), now Earthcare Associates

Dr. James Reis, Earth Data Corporation

San Diego County Archaeological Center

University of California at Los Angeles (UCLA) Archaeology Laboratory

Dr. Andy Yatsko, Cultural Resources Program Manager, Navy Region Southwest.

EXECUTIVE SUMMARY

The research presented in this report has generated protocols for the archaeological inventory of large areas using synthetic aperture radar (SAR). These protocols are provided here, as well as the manner in which some of them can be applied to multispectral data sets. The protocols were expanded in this way because the experimental SAR platform that collected the data originally used in this research, was decommissioned before the conclusion of this research, The experimental platform was (AIRSAR), owned and operated by the NASA Jet Propulsion Laboratory at the California Institute of Technology (JPL/NASA), The expanded protocols utilize SAR data that is available from commercial providers, *and* commercially available IKONOS multispectral satellite data. Combining a vector that was produced from the multispectral data set with the vectors created from the single usable SAR band obtained from the private sector was enough to compensate for the loss of the vectors that we had produced from the three AIRSAR bands. That is, signatures developed from the private sector data sets were as accurate as those generated by the AIRSAR data sets.

Our research was conducted from 2002-2005, and was made possible by a grant from the Department of Defense's Strategic Environmental Research and Development Program (SERDP) (SI-1260) The test area was San Clemente Island, California. Protocols rely upon algorithms to merge data from multiple flight lines, collection of spatially precise ground data with which to develop signatures, knowledge of site morphology, and elegant statistical treatments of sensing device return values to automate the development of site signatures (in contrast to using the "trained eye" of remote sensing experts).

The Introduction of the report presents the study rationale, SAR basics essential to this research, study site description, and an overview of fieldwork done. The Methods section details eight SAR methods that were developed: data collection, including look angles, flight lines, and choice of band and polarization; data processing and image production, including orthorectification and the merging of data from multiple flight lines; image analysis (post-processing), including statistical techniques and iteration of images; corroborative use of multispectral data sets; spatial modeling; procedures for incorporation into, and analysis with, Geographic Information System; establishment of statistically based site signatures; and procedures for ground verification. In a Discussion, the authors extend some of their findings to archaeological research at San Clemente Island, where the archaeological record covers a period of almost 10,000 years.

The report concludes by highlighting some important management implications for the use of SAR as an archaeological evaluation tool for sizeable land areas. Practical application of these protocols will greatly reduce the cost, and time, of not only archaeological site inventory, but also of identifying areas that are cleared for any type of development or training use, as well as those that should be preserved for scientific or historical purposes. The protocols can be used in most arid and semi-arid regions, notably in the western United States, where numerous military and Department of Energy lands are found, but also in other such regions around the world where the United States government is the steward for cultural resources.

1. INTRODUCTION

1.1. Project Background and Objectives

This report presents methods for using airborne synthetic aperture radar (SAR) in the inventory of archaeological sites. The research was conducted on San Clemente Island, California with funding from the Department of Defense's (DoD) Strategic Environmental Research and Development Program (SERDP) as project SI-1260. SAR data were collected by the Jet Propulsion Laboratory/National Aeronautics and Space Administration (JPL/NASA) platform Airborne Synthetic Aperture Radar System (AIRSAR) and the private sector platform Geographic Synthetic Aperture Radar (GeoSAR).

The problem that the research was intended to address can be stated succinctly: *The presence of unidentified and unevaluated archaeological sites (and other cultural resources such as historic sites in ruins) on United States DoD land (and on lands administered by other federal agencies, e.g., the Department of Energy) poses the continual risk of costly delays in training, testing, and construction.* In particular, approximately 19 million acres of DoD land remain to be surveyed, with evaluation and mitigation required before disturbance. Numerous Phase I cultural resource surveys (Identification) and Phase II research projects (Evaluation) are conducted each year as required by the National Historic Preservation Act of 1966, as amended. In fact, at many areas managed by the military there has been an effort to accomplish a 100% inventory and evaluation. However, conventional inventory methods are very costly, at $30 to $35 per acre, and evaluation costs average more than $15,000 per site.

What is needed are ways to accurately and rapidly inventory wide areas using noninvasive, nondestructive technologies that do not involve artifact collections. SAR has for years held out the promise of a cost-effective way to find archaeological sites and thus to alleviate these problems. SAR collects a series of radar echoes over a study area from a moving platform such as an airplane or a satellite, thereby creating a synthetically large antenna that produces high-resolution images of landscape features. Until the current project, however, methods for the application of SAR to survey and evaluation of large areas had not been developed. The purpose of project SI-1260 was to develop such methods.

In the remaining parts of the Introduction, a brief background on the use of SAR and then describe the research test area and give an overview of the fieldwork that was completed will be provided. In the second major section the primary results of this study: eight methods for applying SAR in archaeological evaluation, is presented. In the third section implications of findings for archaeological research at San Clemente Island and elsewhere is discussed. In the fourth section the practical management and research implications of findings is considered.

1.2. Basics of SAR

Most aerial and satellite remote sensing systems are passive. As enormously informative as passive sensing devices are, radar is an active sensing system uniquely capable of sensing physical, as opposed to chemical, aspects of the environment, and thus for detecting *physical* aspects of environmental change that are associated with human occupations.

Radar is an acronym for "Radio Detection and Ranging." A radio device transmits pulses of energy, in the form of microwaves, and then maps distance based on the time it takes for return

pulse to arrive at the device. The device determines the wavelength of the microwave, the polarization of the microwave (which can be either horizontal or vertical), and its strength. Some radar devices can transmit more than one microwave band. Materials that radar microwaves encounter affect the return pulse differently, depending upon what they are made of (especially the dielectric property of the material), their shape, and orientation to the pulse. Resolution of images created from radar data can be increased by increasing the size of the antennae that transmits the microwaves, the larger the antennae, the higher the resolution. Synthetic aperture radar (SAR) creates a virtual, very large antenna by moving a real antenna at high speed. The faster the movement of the antenna, the larger the virtual antenna, and the higher the resolution of radar images produced from collected data.

SAR systems have been carried by both space and aerial platforms. Space-borne synthetic aperture radar systems have been used to map over 80% of the earth by means of the Shuttle Radar Topography Mission (SRTM). This application provides an example of how effective SAR is in providing high resolution over large areas from a platform at a high altitude.

SAR systems carried on airplanes deliver, as one might expect, both higher resolution and higher signal-to-noise ratios than do those carried on space platforms. Also, the ability to carry radar instrumentation along several flight lines results in multiple observation geometries, providing multiple image perspectives. This can be used to overcome a serious problem in the interpretation of radar images and data: shadowing. Because radar is an active sensing technology that illuminates the ground surface at an angle, radar “shadows” form on the far side of hills, ridges, and in fact, anything that reflects radar waves.

To fill in the data gap that produces the shadow, the surface must be illuminated from another direction, or perhaps from even more than two directions. Multiple illuminations produce several images, each having areas of no data unless they are merged. Software developed during this research project does just that: it merges data collected during multiple flight lines, thereby mosaicking the imagery produced from the data.

The JPL/NASA AIRSAR, flown on a retrofitted DC-8 jet, was one of the platforms utilized in this research project. AIRSAR can provide multiband and multipolar SAR data from which high-resolution imagery can be produced. In addition, AIRSAR utilizes more radar bands and polarizations than any other air- or space-borne radar device known to the principal investigators. Therefore, AIRSAR was suited perfectly to this research, which was intended, in part, to identify those bands and polarizations that will be most useful to archaeological site inventory and evaluation. The other SAR platform that provided data to this research, GeoSAR, represents the migration of technology developed by NASA to the private sector. In the future, such platforms will supply data required for the application of the methods in this report.

SAR returns are influenced largely by four phenomena, each of which is implicated in human alteration of the environment: topography, structure, surficial roughness, and dielectric property.

The first of these, *topography*, influences environment at a basic level; and environment patterns human settlement. Thus, topography influences settlement pattern in an elementary way. Prior to the advent of architecture, topographic irregularities such as ridges, hills, caves, and ledges offered shelter to human populations. They also formed diverse econiches for, in turn, a varied species of plants and animals that, in turn, encouraged human occupation.

Topography is the key to understanding hydrology, and water is the most important human attractor. Looked at another way, water is arguably the most important limiting factor

determining human settlement patterning. In turn, human occupation of the landscape produced topographic change on scales from micro to macro. Humanly designed structures can be thought of as a kind of topographic change. Often, humans worked to enhance landscape characteristics that provided suitable habitats to plants and animals that were useful, thereby gradually altering topography. In most areas, this occurred long before formal agriculture is introduced.

Structure as the term is used here refers to formal angular geometric form. Such structure is found, for example, in architecture and vegetation. Some structural forms are more easily detected by radar than are others. Radar is not well reflected by spherical objects. Rather, radar highlights angles and corners, and it is especially sensitive to angular constructions, either made by humans or occurring in nature.

Radar waves can be used in ways that detect structures of differing orientations. Radar waves can be polarized either vertically or horizontally. Some polarizations are reflected well by vertical structures and poorly by horizontal structures, while the reverse is true of other polarizations. Because AIRSAR uses three bands that can each be polarized in four different ways, the spectrum of returns from any given target (e.g., species of vegetation) can be used to formulate a signature based upon the physical structure of the target. *Surficial roughness* can be characterized similarly. Polarized shorter waves (C- and L-band in the case of AIRSAR) often provide the best results here. However, structure and roughness reflect radar waves differently. Given this, it is possible under certain circumstances to determine what target characteristics have produced radar returns. This will be discussed in more detail later.

Radar is also returned differentially based upon *dielectric property* (measurable responses of a material to electric fields). Often, variations in dielectric property in the field are related to soil moisture, although other attributes, such as conductivity of material, can affect return. It is sometimes possible to determine which returns have been produced by dielectric properties, as it is with returns from surficial roughness and structure. The SAR data sets used are seen in Table 1.

Instrument	Frequency band	Bandwidth (MHz)	Band Length (cm)	Single-look range resolution (m)	Polarizations	Interfero-metric	Pixel Size in This Study, After Orthorectification and Post-Processing
AIRSAR	P	20	68	7.5	HH, VV, HV, VH	No	5,5
AIRSAR	L	40, 80	25	3.7, 1.8	HH, VV, HV, VH	Yes	5,5
AIRSAR	C	40	5.7	3.7	HH, VV, HV, VH	Yes	5,5
GeoSAR	P	160 (max)	86	0.9	HH, HV	Yes	N/A
GeoSAR	X	160	3	0.9	VV	Yes	3,3 DEM 5,5 Image

Table 1: **Radar bands and polarizations used in this research**

1.3. Research Test Area and Overview of Fieldwork

San Clemente Island lies approximately 60 miles off the coast of southern California (see Figure 1). The geomorphology of the island is best described as a series of marine terraces culminating in a high plateau, and vegetation tends to be grasses and small shrubs. The island was selected because it contains a wide variety of archaeological sites and a set of environmental zones that are representative of those found in the western United States (in which DoD and the Department of Energy, among other federal agencies, own large tracts of land for which they must provide environmental stewardship).

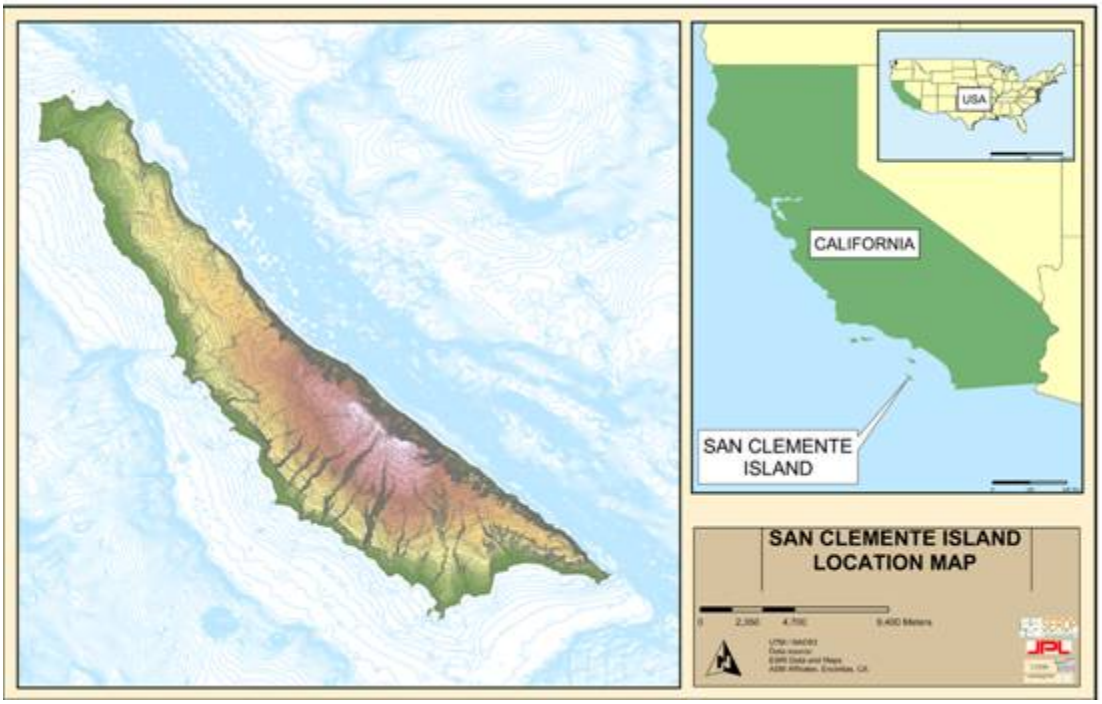

Figure 1: Test area: San Clemente Island

San Clemente Island was also selected because excellent baseline data exist for the island, including precise locations and characterizations of many archaeological sites, as well as environmental information, including accurate topographic, hydrological, soil, vegetation, and geomorphology characterizations. These baseline data were collected by Dr. Andy Yatsko, Cultural Resource Manager for Navy Region Southwest (Yatsko, 2002). Dr. Yatsko made numerous contributions to this research throughout its four-year duration, utilizing his comprehensive knowledge of the archeology and the environment of the island.

AIRSAR collected data over San Clemente Island on 7 April 2002 utilizing different look angles and modes. This was done to establish the first of the methods listed in the next section, that is, to determine the optimal manner in which SAR data should be collected to best discover archaeological sites. Four field sessions were conducted in 2003, five additional field sessions were conducted in 2004, and three in 2005. Ground control points (GCPs) using sub-meter accuracy differential processing geographical positioning system (DGPS) equipment collected during 2003 and 2004 field sessions were used not only for signature development, but more

immediately to determine the spatial precision of images produced from orthorectification methods. GCPs were initially collected by Cultural Site Research and Management, Inc. (CSRM) at four survey plots (see Figure 2), each located in a separate environmental zone on San Clemente Island. Later, additional GCPs were obtained from the Navy Southwest Regional Office through Dr. Andy Yatsko, Cultural Resource Manager for that region. Finally, other GCPs were collected by CSRM, most of these in the Coastal Terrace Geomorphological Zone. This is a small band of land on the western side of San Clemente Island, where soils and general environmental conditions are quite different than elsewhere on the island. In great part this difference is due to the salts introduced by the nearby ocean. In all, 100 sites were recorded to sub-meter accuracy in the Coastal Terrace Zone, while 733 sites were collected on the rest of the island. GCPs were collected not only for the center point of each site within each survey plot, but in many cases also for site features that might affect the radar return from each site. Therefore, in most cases, not only were highly accurate points recorded by means of DGPS units for these sites and features, but also each site and feature was delineated with a DGPS, forming a polygon that could be retrieved as a layer in the Geographic Information System (GIS) for San Clemente Island GIS. Once images were produced through processing at JPL, they were post-processed at CSRM in ways that facilitated development of signatures for archaeological sites.

Figure 2: Initial survey plots, located in representative geomorphological zones

The chart in Figure 3 provides a summary representation of the work flow over the four-year extent of the project. In presenting the eight SAR methods that were developed in the research in the next section, which provides a more detailed examination of separate aspects of the project.

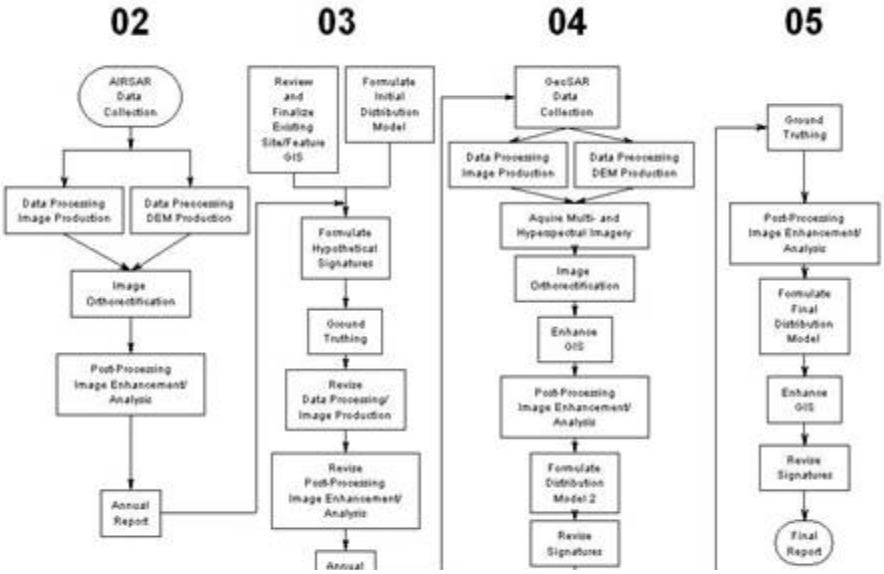

Figure 3: A summary representation of the work flow over the four-year extent of the project

2. METHODS: EIGHT SAR METHODS

2.1. Method 1: SAR Data Collection: Look Angle, Mode, and Optimal Flight Lines

2.1.1. Look Angles and Flight Lines

Optimal data collection is accomplished by means of *complementary look angles.* All SAR platforms illuminate the area to be examined by means of transmitting electromagnetic waves of microwave length. Only object planes facing in the direction of the transmission are illuminated and subsequently sensed, with other surfaces remaining undetected and thus not subject to characterization until illuminated from the proper angle. Complementary look angles are produced by executing flight lines from different sides of the area to be examined. Ideally, this would be done by scanning the same area from the north, south, east, and west. Depending upon topography; however, only two or three angles might be required. At San Clemente Island, a racetrack flight plan that provided three different look angles worked very well.

2.1.2. Choice of Band and Polarization

AIRSAR provides optimal SAR versatility by utilizing three different radar bands—C, L, and P—that can be polarized either vertically or horizontally when transmitted or received. No other SAR platform provides this many bands that can be polarized. This multipolar, multiband toolkit can be instructive about a great variety of features that might be found on a landscape because each band is scattered when it encounters features as small as one-fourth of the band's wavelength. For example, the approximately 5.7 cm in length C-band (all band lengths given in this report are for AIRSAR and GeoSAR) can provide great detail about small structures that are often associated with landscape roughness, such as that produced by gravels or small rocks. Vegetation can also scatter 5-cm wavelengths, allowing differentiation, for example, of grasses from shrubs. The L-band, 25 cm in length, reacts noticeably with landscape features that produce variation in gross texture, such as large stones or small boulders, plants on the scale of tall grasses, medium to large shrubs, and trees. P-band, about 68 cm in length, interacts with larger features such as human-made structures, boulders, and trunks of very large trees. However, depending on its polarization, the megahertz at which it is transmitted, and the water content of material that it encounters, P-band can at times pass through the trunks of all but the largest trees. The available private-sector aerial SAR platforms, notably GeoSAR (which was designed by JPL), carry, at most, P- and X-band (X-band length is 3 cm). P-band can polarize in two ways, as compared with AIRSAR's four, and X-band is polarized only vertically for both transmission and reception (VV) (as seen in Table 1).

Because use of the P-band can interfere with television and citizen's band radio, only the AIRSAR C-band and GeoSAR X-band are routinely deployed and analyzed interferometrically to produce digital terrain models (DTMs) or digital elevation models (DEMs). Because these are short wavelengths, the radar signal may not penetrate to ground surface. However, at sites such as San Clemente Island with sparse vegetation comprised of grasses and small shrubs, some X-band and C-band radar penetration to the surface is likely, and longer wavelength radar waves may penetrate through the vegetation and into the ground surface (see for example Henderson and Lewis, 1999: 36, 163).

The most informative radar band polarization will depend upon the structural characteristics of the sites to be found and the general environment of the area to be examined.

At San Clemente Island, for example, we see strong evidence that both C- and L-bands interact with the rock scatters associated with the presence of archaeological sites. They may also be reflected by grasses and brushes that are anomalous to surrounding vegetation. Soils created by human occupation often attract distinctive sorts of plants, which frequently grow with more vigor than do those surrounding them. These soils, in general, and by observation on San Clemente Island, are richly organic, ashy, and contain rock, stones, shells, and artifacts. These soils tend to clump, creating interstices that fill with water. Interstices between material introduced by human occupation (e.g., rock, shells artifacts) also fill with water. Water soaked soils are highly conductive to electricity. The strongly conductive properties of midden soils on San Clemente Island reflect those radar bands that penetrate overlaying vegetative layers. More specifically, P-band returns are of a magnitude that suggests the manner in which a flashlight in a dark room interacts with a mirror on the floor at an angle. While the cone of light that strikes its surface illuminates the mirror, most of the electromagnetic waves skip from the surface and off into space. The return is relatively weak. The phenomenology of the P-band in its interaction with the typical archaeological site on San Clemente Island follows this model. To the P-band, the site acts much like a mirror, as seen in Figure 4.

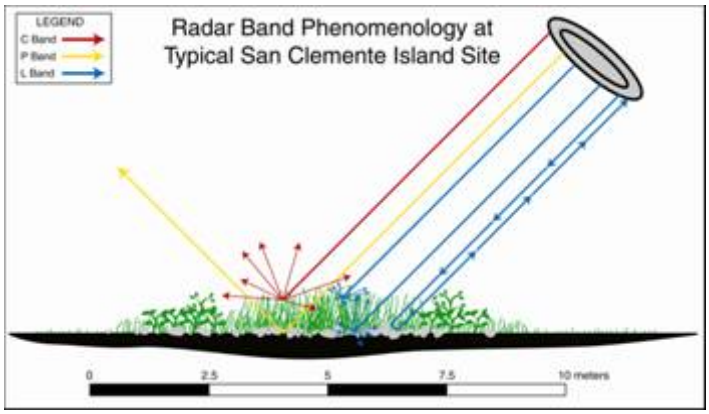

Figure 4: Schematic of radar wave phenomenology at typical San Clemente archaeological site

Signature development for archaeological sites, approached scientifically, demands some prior knowledge of site morphology. As is true in general, we must know what we are looking for before we can hope to find it. The more known about the physical and chemical attributes that comprise the site, the better. Therefore, background research that either draws from prior fieldwork or collects information about site morphology by means of preliminary fieldwork is essential to the methods that are developed in this report: the typical sorts of archeological sites must be determined in order to provide the universe of values from which signatures are created. Similarly, the radar bands used should be selected on the basis of what is known prior to the investigation about the structure and physical characteristics of archaeological sites in the inventory area. As to mode of polarization, structures that are marginally detectable because of their spatial orientation by bands of a certain wavelength are generally more detectable in cross-polar mode. It is this versatility inherent in the AIRSAR platform that made it the best choice for the determination of the value of polarization to the current application. While the shorter wavelengths proved to be most valuable in directly detecting archaeological sites at San Clemente Island, this might not always be the case. In other areas, sites are to be found beneath soils or under forest canopy. For example, on a spin-off project, using AIRSAR in Central America on mostly Mayan sites, initial findings are that masonry features located beneath even a tropical rain forest canopy can be detected by the unnotched P-band polarized vertically and transmitted at 40 MHz, higher than would have been done near developed areas (Comer et al., 2005).

2.2. Method 2: SAR Data Processing and Image Production

2.2.1. Orthorectification

It became apparent early in this research that in order to fully exploit the capabilities of SAR to detect archaeological sites, images would have to be rigorously orthorectified. Previously, research utilizing radar imagery had been focused on very large features, often long and linear, or on areas that were generally homogenous in regard to broad taxonomic categories of interest, for example broad agricultural areas, geomorphologic zones, large ice sheets, and oceanic wave patterns (e.g., Moghaddam, M, 2001; Schmullius and Evans, 1997; Durden, et. al., 1989; Crippen and Blom, 2000; Gabriel, et al., 2000). To find relatively small archaeological sites, a much greater degree of precision was necessary. The most common sites on San Clemente Island, the habitation sites, are on average 9.2 meters in diameter. Because most radar imagery was made up of 5-meter square pixels, it was obvious that spatial accuracy would be imperative. (The statistical approach described later also made the use of relatively large pixels feasible.)

2.2.2. Merging Data from Multiple Flight Lines

It was necessary that radar imagery be available for all locations within the survey area. To accomplish merging of data from multiple flight lines, JPL radar engineers developed what they dubbed “Jurassic Proc” software (for the gigantic body of data used and the enormous processing power required to produce images) to merge data from two or more flight lines. Interferometric data merged in this way provided a DEM of the terrain that is much more accurate than any produced before. The images orthorectified by means of the interferometric DEM proved to be amazingly accurate. For all of the radar bands utilized by AIRSAR (P, L, and C), an accuracy on the order of 5 meters was obtained. GCP for this test were supplied by a chicken-wire square that had been utilized by San Clemente Island botanists to protect cultivated plants from foraging animals and an approximate figure-eight arrangement of barbed left over from US Marine Corps maneuvers in the area of the island’s old airfield.

2.3. Method 3: SAR Image Analysis (Post-Processing)

2.3.1. Iteration of Image Analysis

Image analysis was conducted numerous times, as described below and as indicated by the diagram in Figure 3. As this diagram indicates, image analysis is a key to virtually all other signature development activities.

2.3.2. Quantitative and Replicable Analysis Methods: Statistical Techniques of Value in Establishing Signatures for Archaeological Sites

The initial attempts at image analysis (sometimes called “image post-processing”) were intended to make archaeological sites more visible in imagery. The first field session in which ground-truthing was conducted revealed, for example, that archaeological sites in certain areas were extremely visible as bright locations in the C-band imagery (single band imagery such as that in Figure 6, is black-and-white; imagery in color is comprised of three bands to which the colors red, green, and blue have been assigned). Having been thus encouraged to examine

imagery, ways to amplify the bright returns that were associated with archaeological sites, not only in the C-band imagery but also in the L-band imagery were developed. Successful enough to enhance imagery so that sites could be identified through examination by trained observers. As can be seen in Figure 5, when L-band imagery produced from the three polarized bands (HH, HV, and VV) was enhanced by means of pixel averaging, the great majority of sites were visible. The most effective method for pixel averaging was the three by three pixel window gamma MAP, or *maximum a posteriori probability* filter (ERDAS, 1997: 199). There are, however, great impracticalities in utilizing this "trained eye" approach. First of all, not all eyes are equally trained. Also, an image may reveal site locations more or less satisfactorily depending upon the peculiarities of the screen upon which it is displayed or the printer that is used to produce a hard-copy image. Brightness is a relative term and is unquantified in the "trained eye" approach.

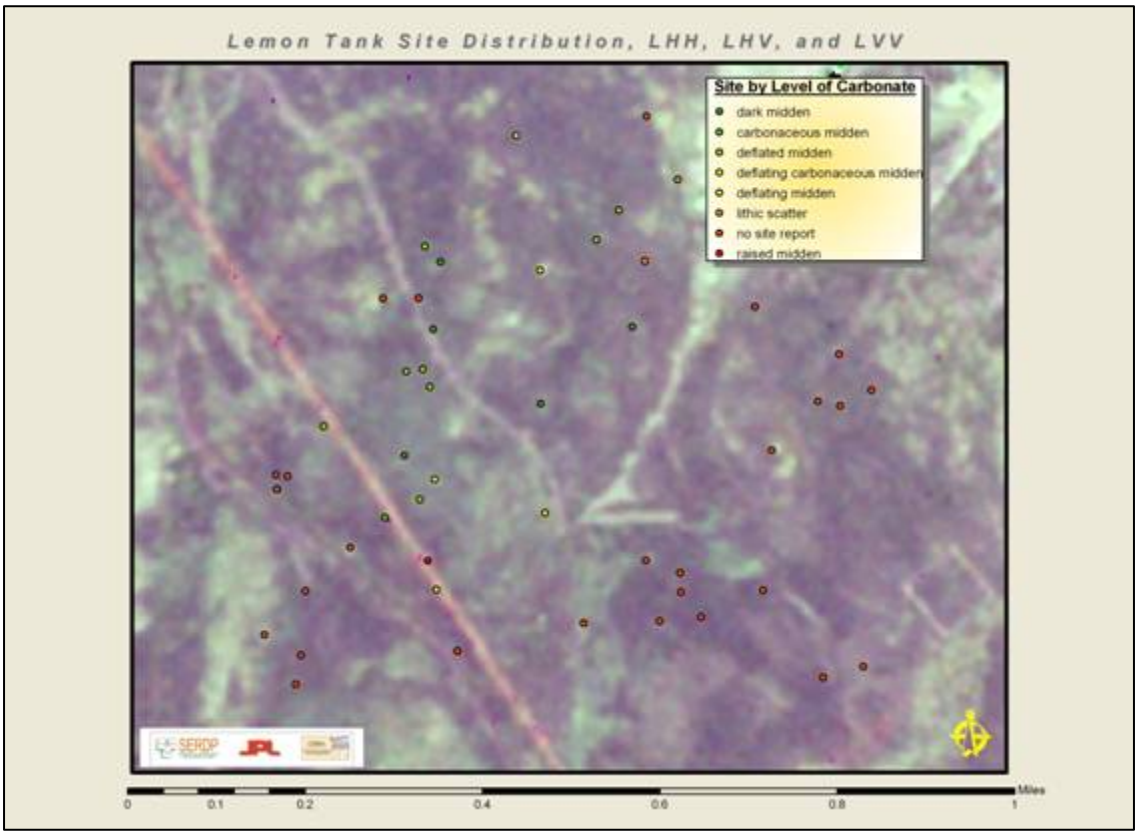

Figure 5: Locations of all known archaeological sites in Lemon Tank survey plot over speckle-reduced radar image

As seen in Figure 6, sites appeared bright in some cases merely because returns from sites were brighter than an unusually dark background. The statistical method, nevertheless, established that although returns from archaeological sites were distinctive, they could be either brighter or darker than immediate surroundings. As can be seen by looking at the histogram of values seen in Figure 6, returns collected from archaeological sites show a central tendency distinctive from that shown by returns collected from the survey area with no archaeological

sites. It is this statistical comparison that can be used to develop archaeological site signatures, rather than the appearance of an image in a given area.

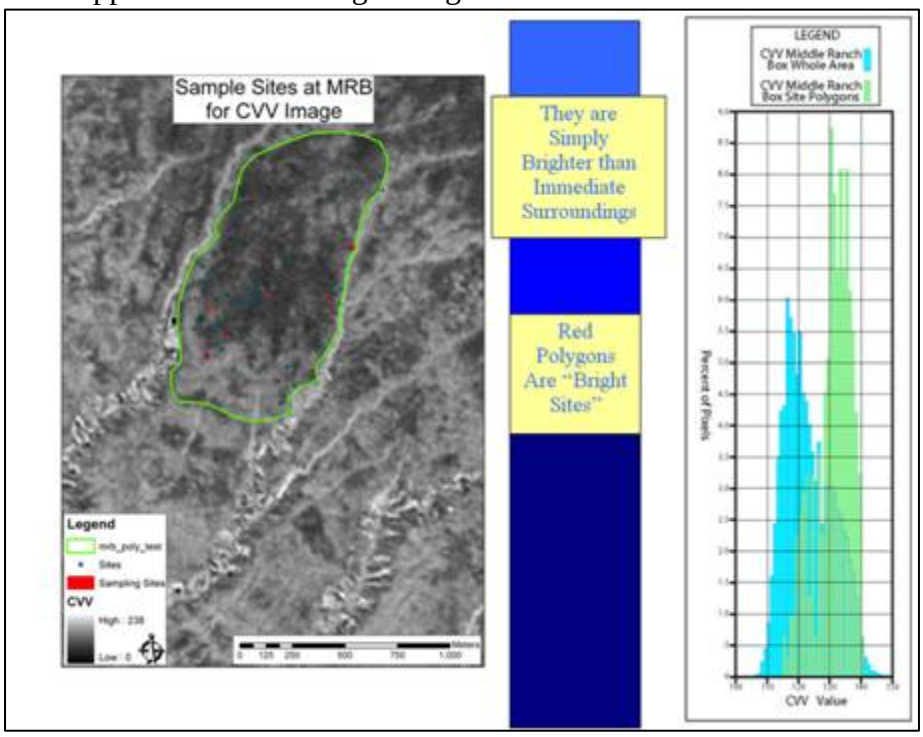

Figure 6: Distribution of CVV returns from site and non-site areas in the Middle Ranch Box survey plot

Statistically, it is an straightforward exercise (although one having numerous steps) to determine whether or not returns from archaeological sites are different enough from returns from the rest of the survey area to conclude, within determinable probability parameters, that the values were taken from two different populations. To do this, a variation of a difference in means test was used. This test was carried out in two steps. The first step was to determine if, simply, there was enough difference between values obtained from the pixels within established archaeological site boundaries and values representative of all pixels not within archaeological site boundaries to justify the conclusion that the two sets of samples actually represented two different populations. The second step was to determine *which pixel values* were most strongly associated with the set taken from archaeological sites. That is, which pixel values were statistically different enough to justify the assertion that they were obtained from a population distinctly different from the rest of the island? Both steps 1 and 2 utilized the following statistical method:

The null hypothesis was that there is no difference between the population of values that lies within site boundaries and the population of values that lies outside site boundaries, that is:

$$H_0: u^1=u^2$$

This was equivalent to testing the hypothesis that the mean of x1–x2 is 0. If the null hypothesis were upheld, of course, it would mean that pixel values associated with archaeological sites could not contribute to signatures for those sites. If, on the other hand, the null hypothesis were disproven, pixel values associated with sites could be used to develop signatures for those sites.

This was tested with the formula:

$$\left(\sum_{n}^{1} x^1 / n\right) - \left(\sum_{n}^{1} x^2 / n\right) < 1.96\sqrt{{\sigma_1}^2 / n + {\sigma_2}^2 / n}$$

Which is to say that the difference of the means of the site and randomly selected samples, or $\left(\sum_{n}^{1} x^1 / n\right) - \left(\sum_{n}^{1} x^2 / n\right)$, will be less than 1.96 standard deviations apart, with the standard deviation of the difference of means being determined by the elementary formula: $\sigma_{x1-x2} = \sqrt{{\sigma_1}^2 / n + {\sigma_2}^2 / n}$ (see, for example, Hoel, 1971: 172).

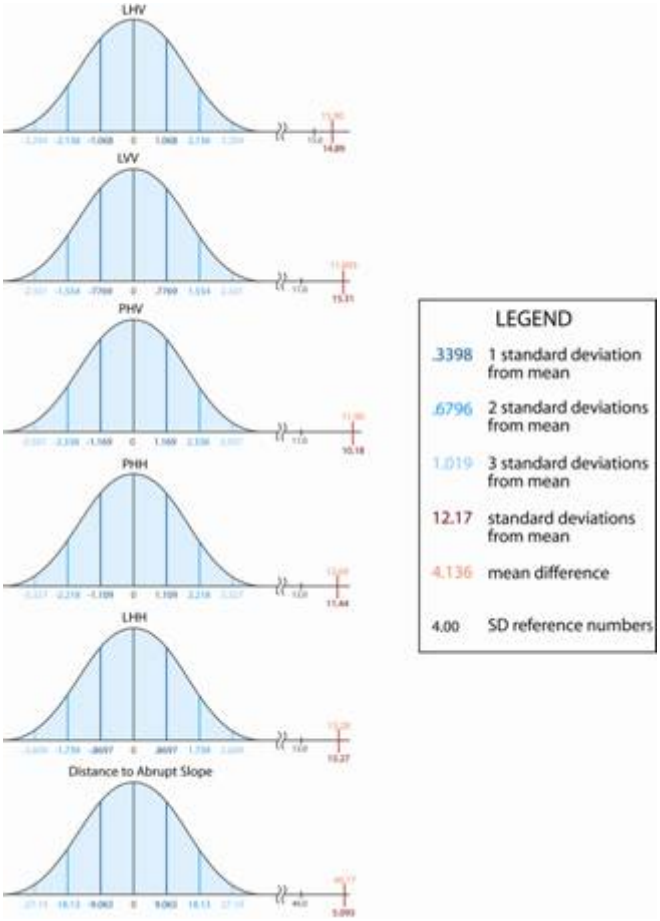

Figure 7: Step 1 difference of means results for several key vectors. Note that site and non-site difference of means are separated by many standard deviations.

2.3.3. Optimal Use of SAR Bands, Polarizations, and Combinations of These

Step 1 results indicated conclusively that, for all vectors[1] tested, values within and outside of site boundaries were drawn from different populations. Figure 7 illustrates some of these results. Note that the difference of means for LHV (which is a L-band transmitted in horizontal polarization and received in vertical polarization) is at 14.89 standard deviations. A difference of 1.96 standard deviations would indicate a 95% probability that the two samples were from different populations. Three standard deviations would indicate a 99% probability that this was the case. The number of standard deviations associated with all of the radar data sets indicated virtual certainty. However, the horizontal polarization of LHH Step 1 test indicated the greatest number of standard deviations, by a small margin, and so this was selected as the most instructive L-band radar vector. This procedure was carried out for all radar bands and

1 A *vector* here is a data set that has been derived from the application of a certain type of remote sensing. In this research, vectors were generated by the use of specific bands and polarizations of SAR; the surface models that were developed from interferometric SAR (including measures of slope); and multispectral returns treated by means of a variety of algorithms (e.g., Tassled-Cap, NDVI).

multispectral standard algorithms (e.g., NDVI and Tasseled Cap) available. The most instructive vectors were determined to be the SAR band polarizations vertically in the C-band (CVV) and P-band (PVV) and horizontally in the L-band (LHH) (from AIRSAR), and XVV (from GeoSAR); slope, derived from interferometric analysis of X-band data (from GeoSAR), and the multispectral vector normalized difference vegetative index (NDVI), calculated from IKONOS satellite (see acronyms, p. v) data. Multispectral data from LANDSAT (see acronyms, p. v) were also used in various protocols.

As a check of this statistical method, it was applied to random samples obtained from areas outside of the known locations of archeological sites. When the null hypothesis was tested for two random samples taken from areas outside of archaeological sites, it was confirmed. As shown in Table 2, results indicated that random samples are indeed drawn from a single population for every vector tested.

Random vs. Random Mean Difference Test

Vector	Rand Stdey 1	Rand Stdey 2	Standard Deviation	mean difference	Rand. Mean 1	Rand. Mean 2	Scaling
CVV	11.51011157	10.31388397	0.5708	-0.9228	127.0410479	126.118261	-1.6165261
LHH	17.33674375	18.02115265	0.9236	-1.8093	125.8912324	124.0818963	-1.958928
NDVI-N	18.01451571	19.02954193	0.9679	-1.6876	235.0855593	233.3980011	-1.7435894
PVV	0.032980673	0.038006617	0.0019	-0.0008	0.134966307	0.134131511	-0.4491392
Slope	7.999462582	8.3211335	0.4263	-0.6238	12.30585348	11.68204118	-1.4631895
XVV	3.808589696	3.97097976	0.2032	-0.2657	-7.528561041	-7.794241331	-1.3073027

Table 2: Statistical tests of two randomly selected sets of pixel values drawn from areas approximately the size of archaeological sites. The results indicate they are taken from the same universe.

The Step 2 statistical analysis utilized the same formula, but it compared the means of all individual pixel values within archaeological site polygons with the means of all individual pixel values within an equal number of randomly selected polygons of equal size. These would be the same if the populations from which values were drawn (i.e., site and random) affected returns in the same way and to the same degree. That is, the null hypothesis in this case would be upheld. The pixels for which the null hypothesis was not upheld would be those that are associated with archaeological sites. In Figure 8, these pixels are highlighted in green. Pixel values for which the null hypothesis is proven are highlighted in red.

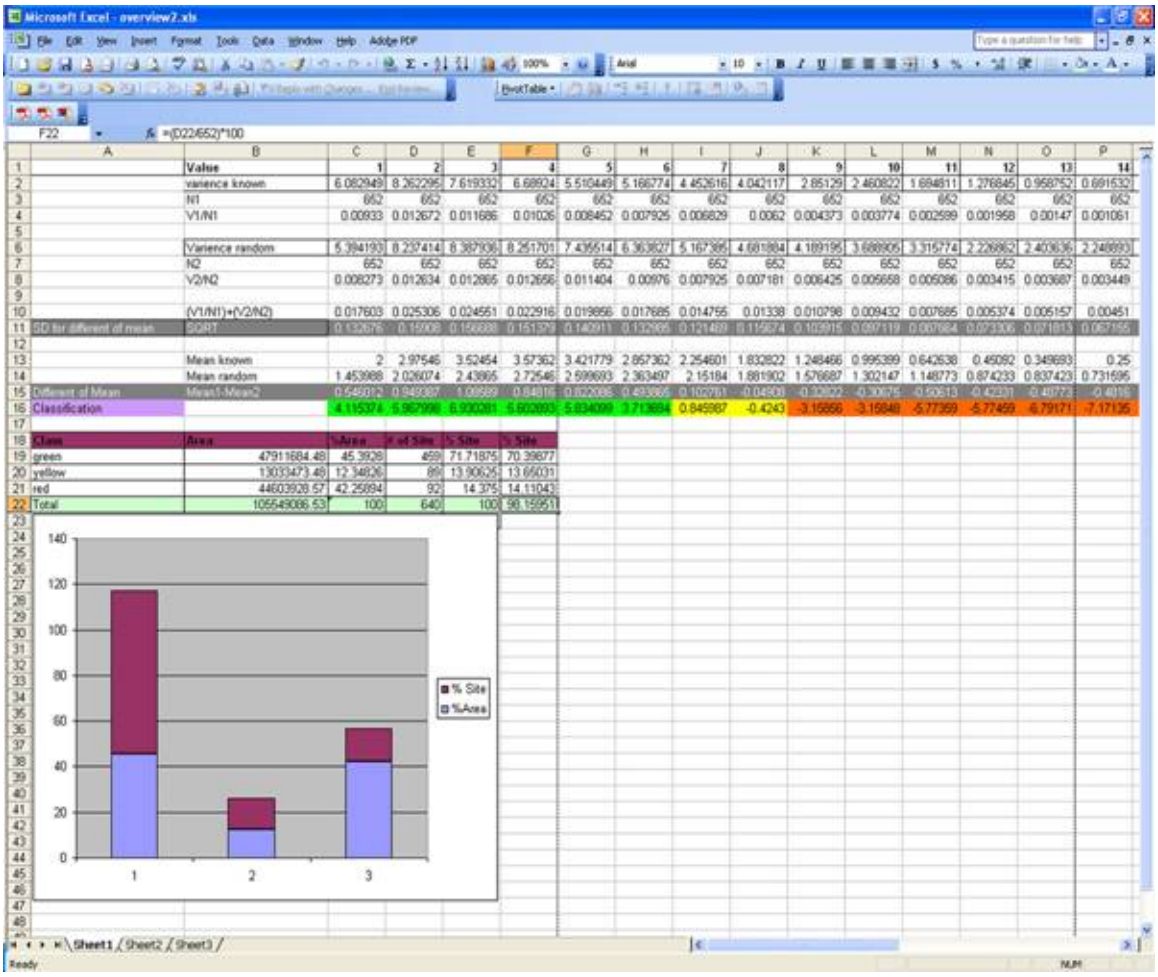

Figure 8: Step 2 calculations: Pixel values more than two standard deviations apart from the null hypothesis mean

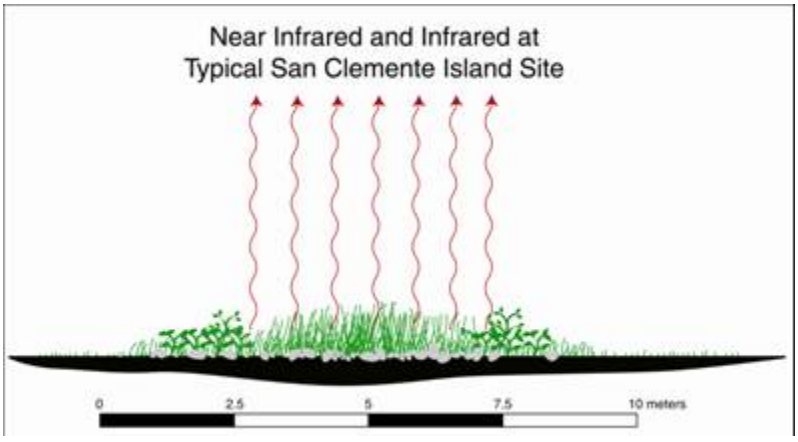

Figure 9: Schematic of NIR and IR radiation at typical San Clemente Island archaeological site

2.4. Method 4: Corroborative Use of Multispectral Data Sets

Certain multispectral image data also correlate very strongly with the locations of archaeological sites. While radar image values were greatly influenced by vegetation structure and dielectric properties, multispectral imagery highlighted spectral attributes of vegetation, including those associated with vegetative health. NDVI values could be used to locate the greener and more vigorous vegetation that developed at San Clemente Island archaeological sites (and typically at non-structural archaeological sites everywhere) by virtue of the enriched, organic soils produced by human occupation. Taken together, then, radar and multispectral imagery were used to sense the following differences (as schematically depicted in Figures 4 and 9).

1. *Topographic roughness produced by the cluster distribution of stone and rock associated with archaeological sites (sensed by SAR)*: This material was probably brought in both for use in erecting shelter and as tools. Given our knowledge of radar wave phenomenology, we can postulate that the L-band is strongly affected by surface roughness of this sort. L-band waves are roughly 25 cm in length. Features that are as small as one-fourth the length of the radar band affect radar waves. This is a dimension that fits with the sizes of stone and rock associated with archaeological sites.

While there are many factors which influence radar backscatter, the Rayleigh scattering criterion is a guide to radar backscattering behavior due to surface roughness (Peake and Oliver, 1971; Schaber, et. al., 1976). Surfaces become rough enough to begin backscattering significant radar energy at approximately 1/4 of the imaging wavelength. Surfaces smoother than this will be dark in radar images, surfaces rougher than this will be increasingly bright. Other key factors include imaging geometry, dielectric constant (largely a function of moisture content), and surface slope.

2. *Vegetative structures associated with archaeological sites (sensed by SAR)*: Vegetation on San Clemente Island is restricted to shrubs or grasses, in part because of scarce precipitation. Vegetation growing on an archaeological site is frequently of a different type than vegetation surrounding it because of soils enriched during human occupation of the site, as well as the presence of rock, shell, and other materials that alter soil moisture and chemical composition. Most archaeological sites on San Clemente Island seem to have at their center grasses. These are frequently either distinct from surrounding vegetation or substantially taller and thicker than any surrounding grasses. The grasses at the center of the site provide a thick biomass structured in a predominantly linear way. The stalks of grass provide a reflector to radar waves, which are scattered differently depending upon their length (short waves seem more readily reflected) and polarization (the strongest reflection results from VV polarization). L-band radar waves seem to be most sensitive to the morphology of archaeological sites. One might speculate that this is at least in part due to the presence of long and tall grasses at the center of many of these sites. Thicker vegetation mass, made up of many individual reflective planes, provides a more effective scattering or reflecting surface than does thinner.

3. *Dielectric property (sensed by SAR)*: Because soils associated with archaeological sites are richer in organic materials than surrounding soils, they are also moister. Soil particles at archaeological sites tend to clump, producing interstices in which water is trapped. This, and perhaps the carbon in the soils from campfires, affects dielectric property, rendering the soil very conductive to electricity. The results of soil conductivity tests at archaeological sites at the old

airfield on San Clemente Island established this quite well. These tests, conducted by Larry Conyers (2000), showed that all sites tested were enormously conductive. This conductivity would affect the propagation of radar waves much as a mirror affects propagation of light waves. Since radar waves are transmitted at an angle, longer waves would be reflected obliquely into space via specular reflection and not back to the radar platform. This is analogous to light from a flashlight striking a mirror obliquely. In both cases, the return from the area illuminated by the beam might be discernable, but would at best be weak.

4. *Greenness and vegetative vigor (sensed by multispectral data)*: As previously mentioned, archaeological soils are conducive to thick and vigorous vegetation. Such greenness and vigor are readily discernible by examination and analysis of NDVI images produced from multispectral data using a standard algorithm.

2.5. Method 5: Radar-derived Spatial Modeling to Detect Archaeological Sites and Features

This research produced statistically based site signatures, not site distribution models. One aspect of spatial modeling, however, that is directly associated with the use of radar data is the surface model, called here the *digital elevation model* (DEM). DEMs were generated by interferometry. A C-band DEM was produced by data collected by the AIRSAR platform, and an X-band DEM by data collected by the GeoSAR platform. The horizontal accuracy of both the AIRSAR and the GeoSAR DEMs, as tested in field sessions at San Clemente Island, was generally five meters or better. Therefore, the merging of interferometric SAR data appears to have been highly beneficial to accuracy, in addition to eliminating radar shadows and resulting gaps in DEMs.

AIRSAR and GeoSAR DEMs were used to generate a slope model with degree of slope being calculated for every 5-meter pixel within the AIRSAR DEM. The GeoSAR DEM that was developed using X-band data as opposed to C-band data provided great height elevation accuracy—about 0.5 meters compared with about 1 meter—due in part to the shorter length of the X-band radar. Also, because this X-band DEM was comprised of pixels of about 3 meters, as opposed to 5 meters for the C-band DEM, slope could be determined for every 3 meters instead of every 5 meters. This more accurate GEOSAR DEM was used to determine those slopes most associated with the presence of archaeological sites. Interferometric DEM data were analyzed utilizing the same Step 1 and Step 2 methods described above. The GeoSAR DEM provided a third and very powerful vector for determining archaeological site signatures.

2.6. Method 6: Procedures for Incorporation into, and Analysis with, GIS

Once the vectors that were very strongly associated with archaeological sites were identified (see 2.3.3, Step 1), they were combined by means of the GIS. A circle was established utilizing the center point of archaeological sites that had been established to less than 1-meter accuracy. Around this center point was drawn a circle with a radius of 15 meters. The average site averaged 9.2 meters in diameter; however, allowance was made for larger sites. Another consideration was that often the effects of site occupation on the landscape were attenuated rather than abruptly ending. The essential rationale for this method was that it was most essential to reliably capture areas that were within site boundaries. The method allowed for a certain degree of spatial error. While this virtually ensured that some areas unrelated to the site would be included in the sample, the statistical nature of the image analysis methods developed from this

research could admit of such dilution of the essential data. Therefore, values were harvested from each of the pixels within sampling polygons. For the control sample, the universe of values known to lie outside archaeological sites, other 15-meter radius circles were established at randomly selected points outside of archaeological sites on the landscape. The statistical tests were conducted utilizing values associated with these two sets of polygons.

2.7. Method 7: Establishment of Signatures Based upon Radar Returns Within Given Environmental and Cultural Zones

Subsequent adjustment of the GIS analytical method (Method 6) was based on iterative episodes of fieldwork and analysis. For example, when an initial test of the signature model was made, it was discovered that the model could predict the location of previously unknown archaeological sites very well in most areas of San Clemente Island. A pronounced exception was the coastal terrace on the western side of the island. In this area, the signatures were much less reliable. Therefore, additional sites were collected to serve as sampling or training areas within what became a separate test area, the Coastal Terrace Zone. Not only did this produce valid site signatures for the Coastal Terrace, but results also improved for the rest of the island. With this in mind, three testing zones, based upon the three major geomorphological areas on the island: the Coastal Terrace Zone, The Marine Terrace Zone, and the Plateau Zone (see Figure 10), were established.

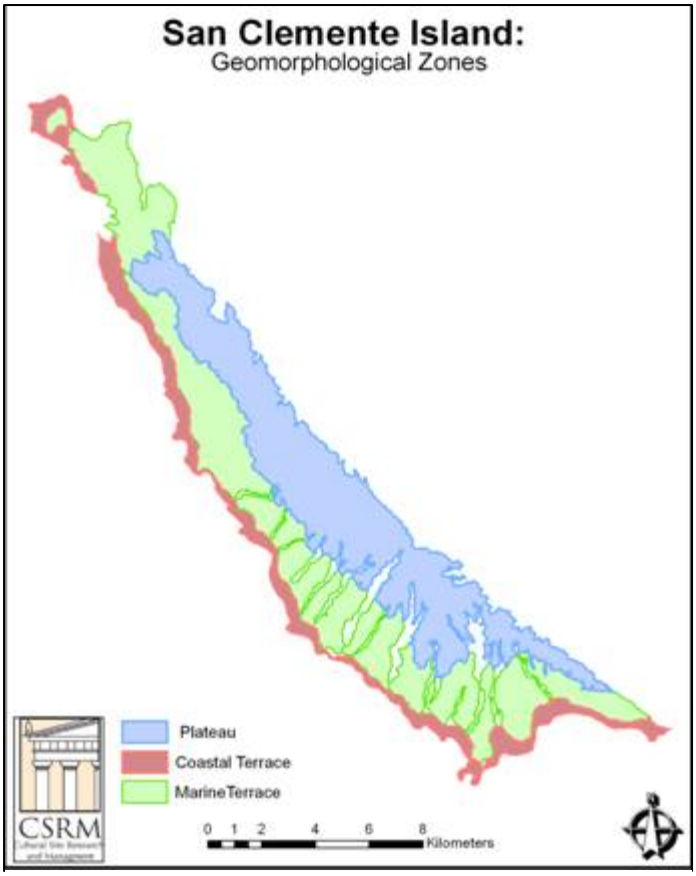

Figure 10: Three testing zones, based upon the three major geomorphological areas on the island: the Coastal Terrace Zone, The Marine Terrace Zone, and the Plateau Zone

Relevant environmental and cultural zones were determined to coincide with previously established geomorphological zones through the iterative process of data collection, field investigation and verification, and additional analysis based on the results of field investigations. This process highlighted data that did not fit comfortably within the existing framework of environmental and site categories, and it recommended reanalysis or reconfiguration of categories. Reconfiguration of categories could not have been accomplished without thorough knowledge of the archaeological record and cultural history of the survey area. Archival research was conducted of sites in excavation records; many of these were obtained at University of California, Los Angeles (UCLA) (Yatsko, 2002).

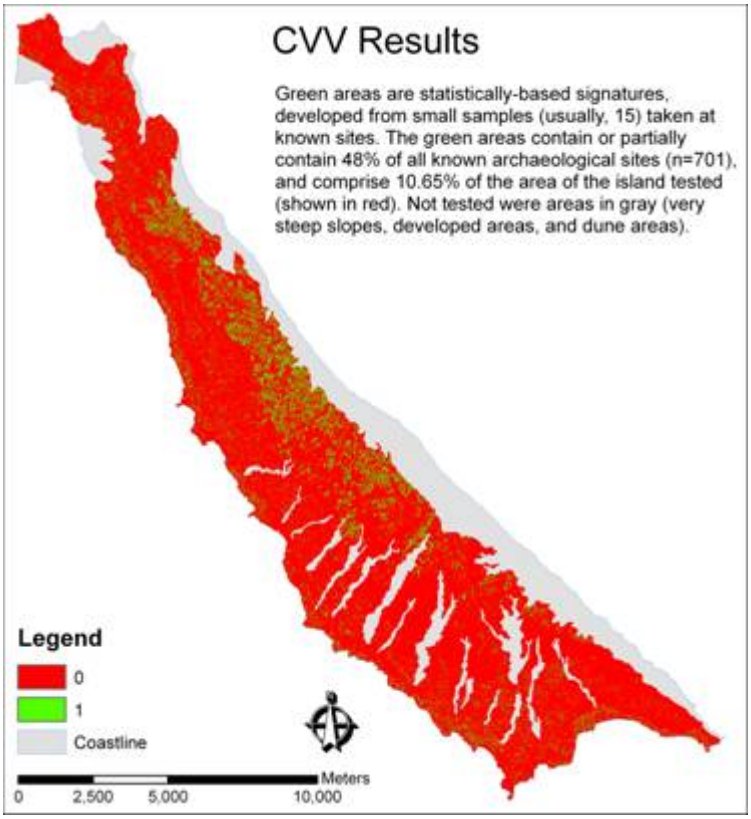

Figure 11: Signatures developed from a single vector (CVV) using a sample of 15 sites.

The *statistically based site signatures* that were developed by the statistical method resulted from quantitative differences in the sensing device returns from archaeological sites, as compared to returns from areas not within archaeological sites. Archaeological site signatures were established using return values from as few as 15 archaeological sites within a given environmental zone. A statistical analysis method developed during this research (see Method 3) was carried out for each site and nonsite pixel value for each vector. Signatures were formed by pixel values that were two standard deviations away from the null hypothesis mean for pixel values taken from vector images for areas within two sets of polygons, the first describing archaeological sites, the second around randomly selected areas not within known archaeological sites. When the null hypothesis is disproven, there is a 95% probability that these two sets of pixels were drawn from different populations. The simplest, and therefore most likely, explanation for the difference of these special sets is that archaeological site characteristics are affecting return values.

An example of signatures developed from a single vector is seen in Figure 11 (CVV Results). Here, by using a sample of 15 sites from each of the three major geomorphological areas, signatures were developed that covered 10.65% of the island, and contained 48% of the remaining 701 sites for which location was known to an accuracy of less than a meter. For the three zones that contributed to this overall result: Using CVV on the Coastal Terrace produced a one-vector signature that occurred over 12.70% of the Coastal Terrace yet caught 64.76% of

sites. When used on the Plateau geomorphological zone, these figures were different. CVV single-vector signatures covered 15.15% of that area and included 49.51% of sites (see Table 3). For the Marine Terraces, these figures were 6.09% and 37.50%. Thus, the local environment played a strong role in how effective CVV was in developing signatures. Table 3 displays these figures for other important vectors, NDVI, for example, is 23.29% and 76.32%.

When different vectors are combined, they produce signatures that are both more reliable, because they are based upon sensing of diverse attributes by the different vectors, and more useful because they pare down the areas that are most likely to contain archaeological sites. Two important applications of this approach are seen in combinations of vectors that would be possible given different research scenarios. For example, if only the AIRSAR platform were available, the results at San Clemente Island would be those appearing in Figure 12. More likely, however, is that future research will have to depend not on data collected by NASA experimental platforms, but on data collected by private sector companies. Fig. 13 shows signature results for data sets available from private sector companies today. These include the SAR aerial platform GeoSAR, and the commercial multispectral satellite IKONOS. GeoSAR carries only X- and P-band. P-band, unfortunately, cannot regularly be used in most of the United States because it interferes with commercial transmissions, including television and citizens band radio. Using only XVV and X-band DEM data, however, it can be seen that results comparable to that obtained with AIRSAR data were achieved.

Plateau				
	% of area	# of pixels	% of sites	# of sites
CVV	15.5	283812	49.51	204
LHH	3.86	72379	35.92	148
NDVI	35.06	657006	80.58	332
PVV	8.06	151065	44.66	184
SLOPE	5.19	97216	38.83	160
XVV	14.2	268986	42.72	176
SUM		1873762		412

Coastal Terrace				
	% of area	# of pixels	% of sites	# of sites
CVV	12.7	74029	64.76	68
LHH	2.65	15441	25.71	27
NDVI	4.78	27890	42.86	45
PVV	24.15	140839	80.95	85
SLOPE	2.89	16836	30.48	32
XVV	18.38	107165	64.76	68
SUM		583100		105

Marine Terrace				
	% of area	# of pixels	% of sites	# of sites
CVV	6.09	128370	37.5	69
LHH	3.05	64220	21.74	40
NDVI	17.95	378202	85.87	158
PVV	16.8	353954	50	92
SLOPE	2.86	60204	34.52	58
XVV	5.23	110318	41.85	77
SUM		2107341		184

Whole Island				
	% of area	# of pixels	% of sites	# of sites
CVV	10.65	486211	48.64	341
LHH	3.33	152040	30.67	215
NDVI	23.29	1063098	76.32	535
PVV	14.15	645858	51.5	361
SLOPE	3.82	174256	35.66	250
XVV	10.59	483469	45.79	321
SUM		4564203		701

Table 3: Key vectors. Note especially column 1 (% of survey area contained within signatures) and column 3 (% of sites falling within signatures).

It should be clear by now that, while some methods apply only to radar data (e.g., protocols for data collection and for data processing to produce images from radar data), others (e.g., the statistical protocols, the use of GIS to merge vectors, ground truthing protocols) were found to be useful for developing signatures from multispectral data sets. Furthermore, there would seem to be no reason why they could not be used to develop archaeological site signatures from hyperspectral and other sorts of data. Notable among these are the statistical methods developed for image analysis (using grid algebra instead of the standard functionalities of image processing software) and methods for ground truthing.

2.8. Method 8: Procedures for Ground Verification of Site Locations

This method for ground truthing was to establish locations of a great number of archaeological sites to a high degree of precision and to acquire highly accurate information about other sites from other researchers. Precise locations for several hundred archaeological sites (particularly in the Coastal Terrace Zone and other areas toward the southern end of the island where this had not been done previously) were collected through physical field work and research and the efforts of other researchers (Yatsko, 2002).

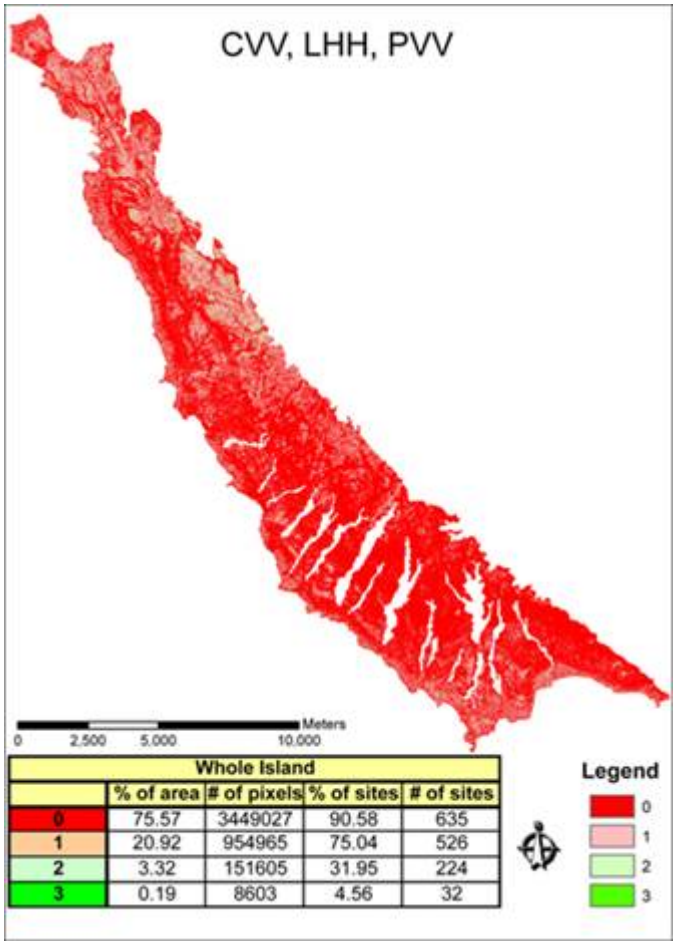

Whole Island				
	% of area	# of pixels	% of sites	# of sites
0	75.57	3449027	90.58	635
1	20.92	954965	75.04	526
2	3.32	151605	31.95	224
3	0.19	8603	4.56	32

Figure 12: Signatures developed from only AIRSAR data

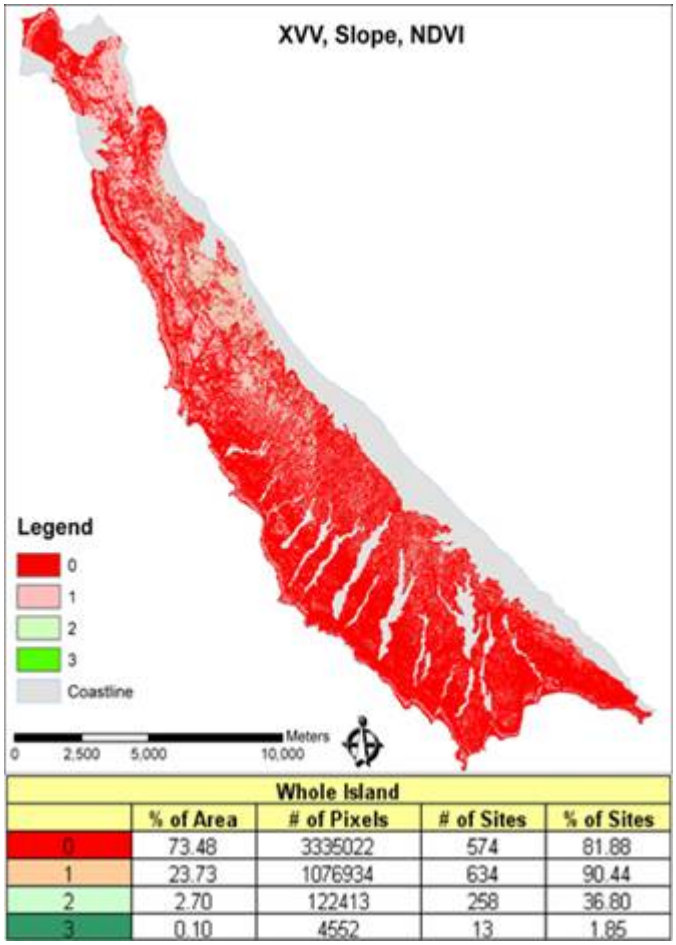

Whole Island				
	% of Area	# of Pixels	# of Sites	% of Sites
0	73.48	3335022	574	81.88
1	23.73	1076934	634	90.44
2	2.70	122413	258	36.80
3	0.10	4552	13	1.85

Figure 13: Signatures developed from private sector airborne SAR and private sector multispectral satellite data

This insured good representation for different environmental zones and provided latitude to alter zone boundaries as suggested by interim results without having to collect many more precise ground control points for other archaeological sites.

Having this store of locational information, sites could randomly be selected within a certain environmental zone (or sites by type, for that matter). A statistical method was used that allowed for the use of relatively small samples (n=15). After developing signatures based on samples, the veracity of the signatures could be tested against the locations of the sites not selected at random.

3. DISCUSSION: APPLICATIONS OF FINDINGS TO ARCHAEOLOGICAL RESEARCH

The research conducted under SERDP project SI-1260 was intended to produce methods for utilizing airborne SAR to find archaeological sites.

There were a number of findings also derived from the data sets and statistical methods developed that are relevant to current archaeological research interests. In the section below, vectors are regarded qualitatively, in terms of what site characteristics they can be used to determine. AIRSAR and GeoSAR data, as well as data collected by means of other remote sensing devices, contributed in many valuable ways to understanding site distribution at San Clemente Island. To begin with, they shed light on several primary determinants of site distribution that have been well established in all areas worldwide where archaeological site models have been formulated. These include proximity to water, slope, soil drainage characteristics, and, in many cases, aspect. To use the first of these, proximity to water, as an example of how remote sensing data can contribute information to archaeological site modeling, the locations of standing water were identified, using LANDSAT imagery, merely by assigning Band 7 to red, Band 4 to green, and Band 2 to blue. This was effective even in detecting very small "tanks," depressions in ravines where water collects naturally.

The accurate DEMs from AIRSAR and GeoSAR data added another dimension to understanding site distribution by forming the basis for a prediction of flow accumulation. The flow accumulation model shows where water would be likely to collect given the current topography. If we assume that the topography is not much changed over the approximately 10,000 years during which the island has been occupied, the model could also be used to show where water was likely to collect in the past. Precipitation in southern California is strongly bimodal: one mode is a long period of no precipitation during the late spring, summer, and early fall, and the other a short period in the winter characterized by rain events that are often intense. A flow accumulation model of San Clemente Island is shown in Figure 14, which indicates where water is likely to accumulate during the winter season. This might have influenced site selection during that time of year in ways that were beyond the scope of this research project but might be examined in the future. In societies in which water management systems have not been developed, sites must be within a few hundred meters at most from sources of water.

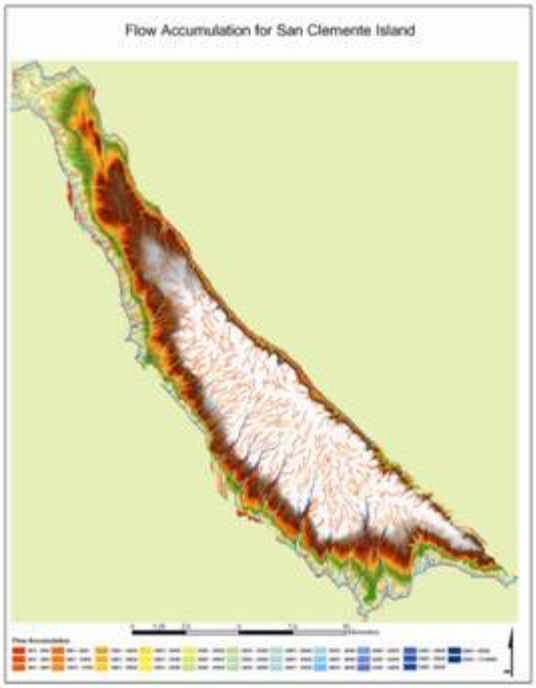

Figure 14: Hydrological flow model, San Clemente Island

The precise AIRSAR and GeoSAR DEMs were also used to model slope. Virtually all occur at slopes of less than 15%. Exceptions, based upon field inspection, appear to be those instances in which erosion is exposing a buried site along the side of a ravine and where a site has been discovered in a cave or rock shelter located in the wall of a ravine or canyon. Further, almost all occur at slopes of less than 5%.

Aspect is also often a strong factor in the determination of prehistoric site selection. Aspect suggests certain functions for the sites found in each of the survey plots. At the northernmost plot, Darter Cactus, 95% of sites are looking to the west (55% SW, 25% W, and 15% NW). These sites are positioned in a way that would provide a view toward the direction of prevailing winds. Wind would move objects of value in the direction of prehistoric occupants of the island (e.g., logs or dead sea animals). By keeping an eye out for materials that were pushed by the wind near the island, these might be collected. Sites also face the Cortez Banks and the channel between the Cortez Banks and San Clemente Island. The Banks provide an environment that has produced a large population of blue whales, and the channel is home to many large pods of dolphin and other sea mammals. Thus, the sites at Darter Cactus might have been lookout spots for pods of sea mammals (Figure 15). That sea mammals comprised a large percentage of the diet of prehistoric islanders is well documented by archaeological excavations on the island. Whales provided not only food, but also many materials that the prehistoric inhabitants of San Clemente Island found extremely valuable. The prime example of this is that whale ribs were used as structural support for dwellings on the island, such as those that have been found in archaeological excavations at the Eel Point and Nursery sites. The Darter Cactus sites could also have served, of course, as locations from which surveillance was kept for valuable items that might wash ashore or come near enough to the island to be retrieved.

Just to the south of Darter Cactus, the Photo Barn survey plot occupies a position on the spine of the island, that is, the highest plateau running north and south. The plateau itself gains elevation steadily as it moves to the south. The aspect analysis indicates that 29.41% of Photo Barn sites face to the west, while 60.8% of sites look toward the east. The sites with an eastern aspect are increasingly blocked as one moves farther east from the prevailing winds, which are northwesterly in summer and more northerly in winter. Yet these sites are located near to places that have a view to the west. Views to the west would have been useful, for reasons detailed above in the discussion of the Darter Cactus sites.

The Lemon Tank survey plot contains many sites that archaeological excavation indicates to have been ceremonial in nature (see Figure 2). These ceremonies seem to have been associated with the Chinigchinich cult, which was a component of what is called in anthropology a revitalization movement. Such movements have been recorded among societies that have been subjected to severe stress. In this case, the social organization experiencing stress would have been the Gabrielino Indians, a group that occupied portions of what is now southern California, including the islands of San Clemente, Santa Catalina, and San Nicholas, at the time of contact with Europeans. Like many Indian cultures, the Gabrielinos lost many members, especially the very young and the old, to European diseases, and more generally to the disruptions precipitated by European contact. These disruptions included conflicts not just between Indians and Europeans, but also among Indian groups as they jockeyed for viable positions in a rapidly and erratically (from their standpoint) changing political and economic environment. Revitalization movements predictably promote group solidarity by appealing to the ancestors to return to earth and restore the order of the past. Ceremonies often involve supplications or other

Figure 15: Viewshed from key San Clemente Island locations to marine resource locations and locations of cultural importance on Santa Catalina Island

communications with ancestors, who are usually thought to occupy locations of geographical prominence, such as hilltops or mountaintops, valleys and caves. Also, ceremonies were intended to draw all surviving members of the group together, more or less under the protective umbrella of the ancestors. At the Lemon Tank sites aspect is toward Santa Catalina Island. This might be expected, as Gabrielinos occupied Santa Catalina Island. The locations of the highest point on Santa Catalina Island and of Two Harbors, a spot on the island where two well protected harbors on the east and west sides of the island almost converge at a narrow isthmus, and the location of the largest historically recorded village on the island, are almost due north of the Lemon Tank sites. The aspect of Lemon Tank sites (24% due north, 20% to the northeast, 24% to the northwest, and in total almost 75% of sites facing generally northward) would suggest that these key points of cultural reference were incorporated into ceremonies held at Lemon Tank sites (see Figure 15). Almost all of the remaining sites, 20%, faced west.

At the Middle Ranch Box survey plot, slightly over 60% of sites again face in a westerly direction (40.38% to the southwest, 19.23% to the west, and 1.92% to the northwest). The predominance of western aspect sites and the large percentage of sites facing the most likely location of sea mammals again suggest the importance of these resources. In this case, we also have a significant percentage of sites with a view to the south (17.31%) and southeast (17.31%), toward other locations on the sea that might provide resources.

This analysis of aspect, which suggests relationships among the sites on San Clemente Island, and even within a universe of sites that includes those on Santa Catalina Island, is made possible because of the high resolution SAR DEM, which was used to create a slope model. This, in turn, was used to map aspect of the terrain on the entire island. It is but one more way, in addition to, among others, the creation of hydrological models; least-cost path analysis; and site proximity to severe slope-- that a precise DEM can be used in archaeological research. These landscape and site models are distinct from the statistically-based signature development protocols presented in this report, but they can be enormously useful in testing research hypotheses. They might, at times, be used, too, in the practical application of the signatures to cultural resource management. For example, research considerations can help to identify which sites are of more potential scientific importance.

4. MANAGEMENT AND RESEARCH IMPLICATIONS

It is obvious that there are numerous management as well as research applications of the research results for San Clemente Island. Almost 37% of sites detected fell within the two vector signatures seen in Figure 13 (the three vectors used here are XVV, Slope, NDVI; therefore, as noted previously, two-vector signatures are those developed by the use of any two of these three vectors), whereas these comprised less than 3% of the area examined. This 2.7% of the land area could be set aside with a high degree of certainty that it contains the locations of many sites. This area could be reduced over time by on-ground survey of that small area of the total landmass in question. One vector signatures encompass over 90% of the sites, and less than 24% of the island. Therefore, 75% of the island could be surveyed relatively quickly, because few sites would be found in those areas. Following this relatively inexpensive survey, most of the island could be cleared for all activities.

If the protocols for collecting, processing, and analyzing SAR and multispectral data we have formulated had been available for a wide-area survey of San Clemente Island before the research we have reported here, we could accomplished the results we have reported for about $150,000. Another way of saying this is that a wide-area, planning level survey for all of the 148 square kilometers (which equals 14,800 hectares, or 36, 572 acres) which comprise San Clemente Island could have been completed for this amount. Thus, this planning level survey would have cost abut $4/acre, or $10/hectare. The survey results could be used to plan the locations of development and training activities.

Whether or not Phase I surveys would be required in the 75% of the island cleared by the wide-area survey results would depend upon negotiations with the State Historic Preservation Officer (SHPO). It is important to note, however, that even if the SHPO stipulates that Phase I surveys be conducted in areas within those cleared by the wide-area survey, these Phase I surveys would cost substantially less than the typical cost of $30 to $35 per acre. This is because the cost of a Phase I survey depends greatly upon how many sites are found. A Phase I survey in environments such as that at San Clemente Island (and, indeed, throughout the western United States) is usually conducted by archaeologists who walk parallel transects at about 20 meter intervals, visually examining the ground surface. When nothing is found, transects are quickly completed, and so many acres can be examined in a day. When sites are found, however, they must be recorded. This is time-consuming, because a an inventory of cultural material (e.g., flakes of stone produced during tool manufacture, shell (by type), tools, material related to structures no longer extant, even fire-cracked rock) must be made, as must a sketch map that shows the locations of cultural materials found and natural features in or near the site. A site form must also be filled out. This is usually begun on site, but typically is completed in the laboratory, which adds more time and expense to the process. Finally, a report is prepared. A report on a Phase I survey that found very little or nothing is quickly prepared, while one that must describe and interpret many sites found can take a great deal of time. Finally, all records (site forms, photographs, field notes) must be assembled according to established protocols for this. Again, if little is found during a survey, this requires little time, but if a considerable number of sites were found, this task, too, requires a significant amount of time. The key to keeping costs down, then, is to conduct Phase I surveys where few or no sites are to be found. This can be accomplished by utilizing the protocols set out in this report to conduct a planning

level, wide-area survey, and thereby identifying areas where sites are extremely unlikely to be found.

Any Phase I survey conducted in areas cleared by the SAR/multispectral wide-areas survey could probably be carried out for no more than $10/acre. To continue to use San Clemente Island as an example, that would mean that even if all 75% of the island indicated by the site signatures to be devoid of archaeological sites were surveyed, this would cost about $274,290. To this would be added $150,000, for the SAR/multispectral wide-area survey, for a total of $ 424,290. This amount, or $11/acre, would them cover the cost of completely clearing 75% of San Clemente Island. In comparison, the cost of a Phase I survey of the entire island at the normal $30 to $35 per acre would range from $1,097,160 to $ 1,280,020.

In considering the cost and management benefits of utilizing these protocols, the following should be kept in mind:

1. Cost estimates for a Phase I survey of the 75% of San Clemente Island indicated by the wide-area survey not to contain archaeological sites will be high, because that 75% will contain areas that have already been subjected to a Phase I survey, and so need not be resurveyed, as well as areas with slopes of over 20%, which are normally excluded from consideration in a Phase I survey, because archaeological sites are extremely unlikely in these areas. For that reason, the $274,290 cost estimate in this case could be used only as an upset limit, with the understanding that payment would be made only for the survey work actually needed, as documented by time sheets.

2. A Phase I survey of the complete 75% of the area cleared during the wide-area survey need not be done immediately, instead, areas can be surveyed as development or training uses are proposed for specific areas. The lower cost per acre for the Phase I survey would still apply. Also, the SHPO might not require a survey of the entire 75% (see below) as Phase I surveys are conduced that corroborate wide-area survey findings.

3. As the wide-area protocols are applied to additional military installations:

a. Costs can be expected to go down for both the wide-area survey and any additional Phase I surveys, as protocols are inevitably improved.

b. SHPOs will become more amenable to the use of wide-area surveys, and will probably not require Phase I surveys in all areas (although they might specify them for certain areas, or for a randomly selected percentage of the area cleared by the wide-area survey).

4. Cost savings for the government go well beyond the immediate saving of approximately $500,000 (or more) in the case if Santa Catalina Island. “Planning around” the areas with site signatures that were developed in the wide-area survey will mean that not only will these sites not be found in a Phase I (which, as noted above, requires significant documentation), but, since such sites will not be disturbed, no Phase II testing will be required in order to comply with NHPA. That testing typically costs at least $15,000 per site (and not infrequently, much more). Cost for Phase II testing does not end with moneys immediately expended for excavation, cataloguing, and curation. Costs continue forever for managing archaeological materials that must be collected during Phase II excavations. Collection management costs include those associated with providing and environmentally-controlled storage space for the materials removed from archaeological sites.

5. The protocols developed here will be useful at many areas in addition to San Clemente Island. They can be used at most arid and semi-arid environments in the western United States.

Cost and management benefits that have been discussed here will expectedly apply equally to these areas.

6. Management benefits can far outweigh even cost benefits at many military installations, where development and training are limited in areas that have yet to be archaeologically surveyed, or where sites are thought likely to be, with or without the use of a predictive model. While the cost savings that can accrue from use of the protocols provided in this report as such installations, removing any possibility of a need to curtail activities important to the military mission is much more important. To return to our test area of San Clemente Island, for a moment, the island has been used by the military predominantly as a target range for naval vessels. This has disturbed archaeological sites only in the immediate vicinity of targets, most of which are located within a fairly small area in the southern portion of the island.. Preservation of archaeological sites has been accomplished by placing signs on them, which notify military personnel not to disturb the ground surface in these areas. Training activity has intensified greatly over the past few years, as the island provides a location and environment that is increasingly useful, and used, for contemporary combined forces training. It is likely that, in the future, merely posting signs on archaeological sites will not be sufficient, and that large areas should be cleared for whatever form training might take.

7. These protocols depend upon the availability of a known set of archaeological sites within the areas for which a wide-area survey is to be conducted. Although it requires only about 15 sites of a specific type (e.g., habitation, lithic scatter) from each major environmental zone within the survey area (at San Clemente Island, there were three), an additional set of sites of each type in each environmental zone is needed to test the accuracy of the signatures. While there are usually a good number of such sites at military installation, at survey areas where these sets do not exist and additional cost will be collection of such sites.

8. An second caveat is that the cost and time required for employing the protocols presented in this report will depend upon the availability of commercial SAR data. There are few commercial SAR platforms at this time. On a brighter note, X-band SAR data sets have recently become available for all of California, as they soon will be for Florida. As time goes on, more areas will be covered. Nonetheless, custom SAR data takes might be problematic from a scheduling standpoint, unless the area for which a wide-area archaeological survey is to be conducted has already been covered by SAR platforms, of unless the SAR platform can collect data as the it moves from other, previously scheduled, surveys. A custom data collection is generally possible, but can be much more expensive than it would be if it fit within of complemented an overall deployment schedule.

9. It is possible that some areas can be successfully inventoried by means of aerial and satellite remote sensing technology as well with data sets other than those collected by SAR platforms. SAR is likely nonpareil in regard to sensing distinct or anomalous structure (e.g., surficial roughness; the mixture of reflecting planes, lines, and angles that can be used to characterize a type of plant or vegetative assemblage; clusters of rocks), yet analysis of LIDAR returns using the statistically-based signature development protocols that were produced during this research might yield comparable results. LIDAR, data, of course, is readily obtained. What LIDAR could not provide is a measure of dialectic property, which has also been useful in signature development, yet other indications of environmental anomaly might compensate for this loss. We have dealt here, for example, with multispectral data, which can isolate vegetative anomaly on the basis of unusual vigor, as opposed to structure. Hyperspectral data very likely

holds even more promise of identifying anomalies that are peculiar or characteristic of vegetative cover that flourished in archaeological soils more readily than in surrounding ones.

As mentioned in Appendix C, the protocols that have been developed under SI-1260 have been found to be eligible for use under the Navy's Broad Agency Announcement (BAA) for Innovative Environmental Technologies and Methodologies. Also, in 2005, two grants were awarded to provide support to efforts to refine these protocols, and to tailor them to other environments. These were a National Center for Technology Transfer and Preservation (NCPTT) grant, *Merging Aerial Synthetic Aperture Radar (SAR) and Satellite Multispectral Data to Inventory Archaeological Sites*; and a National Science Foundation (NSF) grant, *Archaeological Application of Airborne Synthetic Aperture Radar Technology in Southern Mexico and Central America.*

SAB Queries

The SERDP scientific advisory board (SAB) formulated a number of quite specific questions to be addressed in this final report. Although the answers to these might be extracted from the foregoing, for convenience and clarity, answers to the specific questions are provided below:

> *Q1: Explain in your Final Report how high resolution imaging radar, when combined with high resolution Digital Elevation Maps, will significantly improve accuracy and expedite Phase I surveys.*

Answer: Accuracy in identifying the location of archaeological sites was made possible by the Jurassic Proc software, written by a JPL/NASA team supervised by Ronald Blom, and composed of Elaine Chapin, Mahta Moghaddam, and Bruce Chapman. The 2002-2005 research described in this report was conducted during the time when JPL/NASA was completing its oversight of the production of the private sector SAR platform GeoSAR, as well as of the software needed to generate images from the radar data collected by GeoSAR. The radar software team was by then already addressing the need to merge data obtained through multiple flight lines. It modified the software already written to meet the requirement for spatial precision essential to a usable archaeological inventory.

Phase I archaeological surveys will be expedited through the use of the protocols presented in this report two ways: First of all, most military installations are largely inventoried because inventory has been too expensive, time-consuming, and, sometimes, incompatible with military operations. Our protocols involve data collection and fieldwork that can be completed for most installations within one, or at most two, fiscal years, The cost of most inventories will be from $100,000 to $200,000, more or less than this range depending upon the availability of archeological site information with which to develop signatures, the imagery already in hand (some installations might be in possession of suitable SAR or multispectral imagery), and the availability of imagery. The price depends less on the size of the area to be inventoried. Therefore, while a Phase I inventory of a 45,000 acre installation in the western US might cost $1,350,00 to $1,575,000, a wide-area planning level inventory could be conducted with the protocols presented here for only about $200,000.

It bears mentioning that some areas in even those rare installations otherwise completely inventoried for archaeological sites (e.g., Fort Benning, Georgia) have not been inventoried because they contain UXOs or other dangerous materials. Our protocols can be safely used in areas such as this.

Q.2 Discuss the applicability of this technology to other desert and non-desert areas.

Answer: Research funded by NCPTT and just completed by Comer (2006) at Santa Catalina Island, California, provides some indication of the applicability of the protocols to other arid and semi-arid environments. Geomorphologically, the SERDP test area (San Clemente Island) is a series of marine terraces that culminate with a wide plateau. Vegetation consists of grasses and small shrubs. Santa Catalina Island, although located only 31 kilometers to the north of San Clemente Island, provides a very different environment. Instead of a series of essentially level terraces, Santa Catalina Island is characterized by ridges and steep-sides valleys. Santa Catalina Island receives significantly more precipitation than does San Clemente. Vegetative cover is much denser on Santa Catalina Island, and consists of large shrubs, scrub trees, and a good number of large trees. Nevertheless, signatures are roughly as reliable on Santa Catalina as on San Clemente Island. They were effectively developed for both habitation and lithic scatter sites. These signatures were developed with GeoSAR X-band SAR imagery, and X-band DEMs, and IKONOS imagery. The environment at Santa Catalina Island, with severe topography and considerable vegetative cover, is very likely as problematic to SAR as almost any in the western United States. Therefore, the protocols developed here are probably suitable to most places in the western United States. The authors have not tested the SAR or SAR/multispectral protocols in the United States east of the Mississippi River.

Q.3 Discuss the cost per hectare for analysis on various types of land

Answer: As noted above, cost is less dependent upon size than upon:

A) the availability of a suitable number of sites for which the location at the center of the site has been recorded to an accuracy of a few meters (sub-meter accuracy in this regard was obtained for the purposes of this research, but is not necessary here because of the statistical nature of signature development protocols);

B) The availability of data sets (SAR and multispectral). Satellite multispectral data sets are available for virtually every inhabited portion of the earth, but SAR data sets add to survey expense if the survey area is located in areas where SAR data has not yet been collected from airborne platforms, and is remote from areas where SAR platforms are scheduled to collect data

C) The complexity of the environment within the installation. At the test area of San Clemente Island, for example, there were three major geomorphological zones that determined the major environmental zones on the island: Coastal Terrace, Marine Terraces, and Plateau. Availability of water, elevation, and proximity to the saline waters of the ocean were among the factors that dictated soil development and vegetative community. Differences in baseline vegetative cover were especially important to signature analyses, because vegetative anomaly and vigor are secondary indicators of the presence of archaeological sites. Also, vegetative cover can impede SAR penetration to soils, rock, and artifact scatters that are elements of the site itself. San Clemente Island was chosen in part because of its environmental variability. Therefore, one might expect no more than three major environmental zones in a given installation.

The cost for employing the protocols described in this report for a wide-area, planning level survey can be expected to be per $4/acre, or $10/hectare, and these should decrease as the protocols are improved. The factors just above will influence any particular project. For an additional discussion of cost, please see the main section of 4.MANAGEMENT AND RESEARCH IMPLICATIONS

Q.4Discuss how quickly the analysis can be made to allow real-time action to be taken to avoid and preserve the artifacts and sites.

Once the necessary information is in place (site locations, data sets, environmental information), the initial analysis could be conducted within a month. Reporting, in detail, would probably require a bit longer. We anticipate that most projects would take less than one year, and that most of the project time would be spend collecting and verifying the three types of information described above.

REFERENCES

Comer, Douglas, 2006, Merging Aerial Synthetic Aperture Radar (SAR) and Satellite Multispectral Data to Inventory Archaeological Sites. Final report to NCPTT, Natchitoches, LA

Comer, D., Blom, R., Golden, C., Quilter, J., and Chapman, B., 2005, Inventory of Archaeological Sites Using Radar and Multispectral Data. Lecture presented December 2, 2005, at National Geographic Society, Washington, DC.

Conyers, Lawrence, 2000, Field Report of Geophysical Investigations at the Old Airfield, San Clemente Island. La Jolla, CA: Scripps Institution of Oceanography.

Crippen, R. E., and Blom, R. G., 2000. Unveiling the Lithology of Vegetated Terrains in Remotely Sensed Imagery. In *Photogrammetric Engineering and Remote Sensing,* v. 67, pp. 935-943.

Durden, S., J. Van Zyl, and H. Zebker, 1989, Modeling and observation of radar polarimetric signature of forested areas. In *IEEE Trans. Geosci. Remote Sensing* vol. 27, pp. 290-301.

ERDAS Corporation, 1997, ERDAS Imagine Field Guide, Fourth Edition. Atlanta: ERDAS Corporation.

Gabriel, A. G., Goldstein, R. M., and Blom, R. G., 2000, ERS Radar Interferometry: Absence of Recent Surface Deformation Near the Aswan Dam. In *Jour. of Engineering and Environmental Science*, v. VII, p. 205-210.

Henderson, Floyd M., and Lewis, Anthony J., 1999, Principles and Applications of Imaging Radar, Manual of Remote Sensing, Third Edition. New York: Wiley.

Hoel, Paul G, 1971, Elementary Statistics, Third Edition. New York: John Wiley and Sons, Inc.

Moghaddam, M., 2001, Estimation of comprehensive forest variable sets from multiparameter SAR data over a large area with diverse species. In *International Geoscience and Remote Sensing Symposium 2001*, Sydney, Australia.

Peake, W. H., and T. L., Oliver, 1971, The response of terrestrial surfaces at microwave frequencies. Technical Reports No. AFAL-TR-70-301. Ohio State University Electroscience Lab., 2440-7., Columbus Ohio.

Schaber, G. G., G. L. Berlin, and W. E. Brown, 1976, Variations in surface roughness within Death Valley, California-geological evaluation of 25 cm wavelength radar images. In *Geological Society of America Bulletin,* v. 87, p. 29-41.

Schmullius, C.C., and D.L. Evans, 1997, Synthetic aperture radar (SAR) frequency and polarization requirements for applications in ecology, geology, hydrology, and oceanography: a tabular status quo after SIR-C/X-SAR. In *International Journal of Remote Sensing, 18,* 2713-2722.

Sharer, Robert J., et al., 2005. Archaeological Application of Airborne Synthetic Aperture Radar Technology in Sothern Mexico and Central America. NSF grant application, Washington, D.C.

Yatsko, Andrew, III, 2002, Late Holocene Paleoclimatic Stress and Prehistoric Human Occupation on San Clemente Island. Diss. U. of California, Los Angeles

Yatsko, Andrew, III, 2002, Personal Communication

APPENDICES

APPENDIX A

Two sample statistically-based signature values worksheets. Pixel values comprising site signatures are highlighted in green, pixel values that do not contribute to site signatures are highlighted in red.

XVV on Marine Terrace:

Random								
random sqrt	1.032796	1.549193	1.032796	1.046536	1.454058	2.631313	2.455315	2.13809
FID_2	103	104	105	106	107	108	109	110
v/n	0.114755	0.172133	0.114755	0.116282	0.161562	0.292368	0.272813	0.237566
FID_2	103	104	105	106	107	108	109	110
random mean	0.266667	0.4	0.266667	0.333333	0.6	1.066667	1.2	1
Known								
FID_2	197	198	199	200	202	203	204	206
known sqrt	0.258199	0.258199	0.736788	1.437591	1.424279	2.569047	1.799471	2.282438
v/n	0.028689	0.028689	0.081865	0.159732	0.158253	0.28545	0.199941	0.253604
FID_2	103	104	105	106	107	108	109	110
known mean	0.066667	0.066667	0.4	0.733333	0.8	1.2	1.333333	1.933333
(v/n)+(v/n)	0.143444	0.200821	0.19662	0.276014	0.319815	0.577818	0.472754	0.49117
sqrt	0.37874	0.448131	0.443419	0.52537	0.565522	0.760143	0.687571	0.700835
mean-mean	-0.2	-0.33333	0.133333	0.4	0.2	0.133333	0.133333	0.933333
FID_2	103	104	105	106	107	108	109	110
classification	-0.52807	-0.74383	0.300694	0.761368	0.353655	0.175406	0.193919	1.331745
Random								
random sqrt	1.667619	2.772312	2.845213	2.065591	2.963267	3.719959	3.777124	1.791514
FID_2	111	112	113	114	115	116	117	118
v/n	0.185291	0.308035	0.316135	0.22951	0.329252	0.413329	0.41968	0.199057
FID_2	111	112	113	114	115	116	117	118
random mean	0.933333	1.4	1.666667	1.866667	2.733333	2.466667	2.866667	1.266667
Known								
FID_2	207	208	209	210	211	212	213	214
known sqrt	2.390457	3.090693	2.797958	2.939064	1.9223	2.74816	2.604026	2.38647
v/n	0.265606	0.34341	0.310884	0.326563	0.213589	0.305351	0.289336	0.265163

FID_2	111	112	113	114	115	116	117	118
known mean	2	2.533333	3.4	2.933333	2.466667	2.466667	1.733333	1.866667
(v/n)+(v/n)	0.450897	0.651445	0.627019	0.556073	0.542841	0.71868	0.709017	0.46422
sqrt	0.671489	0.807121	0.791845	0.745703	0.736777	0.84775	0.842031	0.681337
mean-mean	1.066667	1.133333	1.733333	1.066667	-0.26667	0	-1.13333	0.6

FID_2	111	112	113	114	115	116	117	118
classification	1.58851	1.404167	2.18898	1.430418	-0.36194	0	-1.34595	0.880621
Random								
random sqrt	1.934647	1.624221	2.086236	2.354327	2.086236	2.144761	1.187234	0.351866

FID_2	119	120	121	122	123	124	125	126
v/n	0.214961	0.180469	0.231804	0.261592	0.231804	0.238307	0.131915	0.039096

FID_2	119	120	121	122	123	124	125	126
random mean	0.8	0.933333	1.266667	1.4	1.066667	1.2	0.533333	0.133333
Known								

FID_2	215	216	217	218	219	220	221	222
known sqrt	1.709915	1.060099	0.703732	0.258199	0.798809	0	0	0
v/n	0.189991	0.117789	0.078192	0.028689	0.088757	0	0	0

FID_2	119	120	121	122	123	124	125	126
known mean	1.266667	0.533333	0.266667	0.066667	0.266667	0	0	0
(v/n)+(v/n)	0.404951	0.298258	0.309996	0.290281	0.320561	0.238307	0.131915	0.039096
sqrt	0.636358	0.54613	0.556773	0.538777	0.566181	0.488167	0.363201	0.197728
mean-mean	0.466667	-0.4	-1	-1.33333	-0.8	-1.2	-0.53333	-0.13333

FID_2	119	120	121	122	123	124	125	126
classification	0.73334	-0.73243	-1.79606	-2.47474	-1.41298	-2.45818	-1.46843	-0.67433
Random								
random sqrt	0.560612	0.258199	0.351866	0.258199	0.258199	0.258199	0.258199	0.516398

FID_2	127	128	129	132	137	139	142	151
v/n	0.06229	0.028689	0.039096	0.028689	0.028689	0.028689	0.028689	0.057378

FID_2	127	128	129	132	137	139	142	151
random mean	0.2	0.066667	0.133333	0.066667	0.066667	0.066667	0.066667	0.133333
Known								

FID_2	223	224	225	226	227	228	229	230
known sqrt	0	0	0	0	0	0	0	0
v/n	0	0	0	0	0	0	0	0

FID_2	127	128	129	132	137	139	142	151

known mean	0	0	0	0	0	0	0	0
(v/n)+(v/n)	0.06229	0.028689	0.039096	0.028689	0.028689	0.028689	0.028689	0.057378
sqrt	0.24958	0.169378	0.197728	0.169378	0.169378	0.169378	0.169378	0.239536
mean-mean	-0.2	-0.06667	-0.13333	-0.06667	-0.06667	-0.06667	-0.06667	-0.13333
FID_2	127	128	129	132	137	139	142	151
classification	-0.80135	-0.3936	-0.67433	-0.3936	-0.3936	-0.3936	-0.3936	-0.55663

NDVI on Coastal Terrace:

Random								
random sqrt	0.258199	0.258199	0.351866	1.055597	0.351866	0.258199	0.593617	0.258199
FID_2	203	204	205	206	207	208	210	211
v/n	0.028689	0.028689	0.039096	0.117289	0.039096	0.028689	0.065957	0.028689
FID_2	203	204	205	206	207	208	210	211
random mean	0.066667	0.066667	0.133333	0.4	0.133333	0.066667	0.266667	0.066667
Known								
FID_2	203	204	205	206	207	208	210	211
known sqrt	0	0	0	0	0.258199	0.258199	0.258199	0.351866
v/n	0	0	0	0	0.028689	0.028689	0.028689	0.039096
FID_2	203	204	205	206	207	208	210	211
known mean	0	0	0	0	0.066667	0.066667	0.066667	0.133333
(v/n)+(v/n)	0.028689	0.028689	0.039096	0.117289	0.067785	0.057378	0.094646	0.067785
sqrt	0.169378	0.169378	0.197728	0.342474	0.260355	0.239536	0.307646	0.260355
mean-mean	-0.06667	-0.06667	-0.13333	-0.4	-0.06667	0	-0.2	0.066667
FID_2	203	204	205	206	207	208	210	211
classification	-0.3936	-0.3936	-0.67433	-1.16797	-0.25606	0	-0.6501	0.25606
Random								
random sqrt	0.910259	0.593617	1.290994	0.833809	1.298351	1.207122	1.125463	0.703732
FID_2	212	213	214	215	216	217	218	219
v/n	0.10114	0.065957	0.143444	0.092645	0.144261	0.134125	0.125051	0.078192
FID_2	212	213	214	215	216	217	218	219
random mean	0.4	0.266667	0.666667	0.466667	0.6	0.8	0.466667	0.266667
Known								
FID_2	212	213	214	215	216	217	218	219

known sqrt	0.593617	0.258199	0.414039	0.258199	0.915475	1.424279	0.617213	0.833809
v/n	0.065957	0.028689	0.046004	0.028689	0.101719	0.158253	0.068579	0.092645

FID_2	212	213	214	215	216	217	218	219
known mean	0.266667	0.066667	0.2	0.066667	0.466667	0.8	0.333333	0.466667
(v/n)+(v/n)	0.167097	0.094646	0.189448	0.121334	0.245981	0.292378	0.193631	0.170838
sqrt	0.408775	0.307646	0.435256	0.348331	0.495964	0.54072	0.440035	0.413325
mean-mean	-0.13333	-0.2	-0.46667	-0.4	-0.13333	0	-0.13333	0.2

FID_2	212	213	214	215	216	217	218	219
classification	-0.32618	-0.6501	-1.07216	-1.14833	-0.26884	0	-0.30301	0.48388

Random

random sqrt	1.889822	1.060099	1.046536	1.032796	0.883715	1.647509	0.833809	1.207122

FID_2	220	221	222	223	224	225	226	227
v/n	0.20998	0.117789	0.116282	0.114755	0.098191	0.183057	0.092645	0.134125

FID_2	220	221	222	223	224	225	226	227
random mean	1	0.466667	0.666667	0.733333	0.733333	1	0.533333	0.8

Known

FID_2	220	221	222	223	224	225	226	227
known sqrt	1.290994	1.387015	1.046536	1.264911	1.253566	0.816497	1.082326	0.941124
v/n	0.143444	0.154113	0.116282	0.140546	0.139285	0.090722	0.120258	0.104569

FID_2	220	221	222	223	224	225	226	227
known mean	0.666667	0.733333	0.666667	0.8	1	0.333333	0.8	0.8
(v/n)+(v/n)	0.353424	0.271901	0.232564	0.255301	0.237476	0.273778	0.212904	0.238694
sqrt	0.594495	0.521442	0.482248	0.505273	0.487315	0.523238	0.461415	0.488563
mean-mean	-0.33333	0.266667	0	0.066667	0.266667	-0.66667	0.266667	0

FID_2	220	221	222	223	224	225	226	227
classification	-0.5607	0.511403	0	0.131942	0.547216	-1.27412	0.577932	0

Random

random sqrt	0.617213	0.48795	1.046536	0.833809	0.617213	0.910259	0.798809	0.63994

FID_2	228	229	230	231	232	233	234	235
v/n	0.068579	0.054217	0.116282	0.092645	0.068579	0.10114	0.088757	0.071104

FID_2	228	229	230	231	232	233	234	235
random mean	0.666667	0.333333	0.333333	0.466667	0.333333	0.6	0.733333	0.533333

Known

FID_2	228	229	230	231	232	233	234	235
known sqrt	0.723747	0.703732	1.175139	1.612452	1.253566	1.76743	0.632456	1.032796

v/n	0.080416	0.078192	0.130571	0.179161	0.139285	0.196381	0.070273	0.114755

FID_2	228	229	230	231	232	233	234	235
known mean	0.666667	0.733333	1.333333	1.2	1	1.533333	0.6	1.266667
(v/n)+(v/n)	0.148996	0.132409	0.246853	0.271807	0.207864	0.297521	0.159029	0.18586
sqrt	0.385999	0.363881	0.496843	0.521351	0.455922	0.545455	0.398785	0.431114
mean-mean	0	0.4	1	0.733333	0.666667	0.933333	-0.13333	0.733333

FID_2	228	229	230	231	232	233	234	235
classification	0	1.099262	2.012709	1.406602	1.46224	1.71111	-0.33435	1.701018

Random

random sqrt	0.941124	0.899735	1.175139	1.032796	1.676163	1.726543	1.099784	1.046536
FID_2	236	237	238	239	240	241	242	243
v/n	0.104569	0.099971	0.130571	0.114755	0.18624	0.191838	0.122198	0.116282

FID_2	236	237	238	239	240	241	242	243
random mean	0.8	0.666667	1.333333	0.933333	1.333333	1.533333	0.933333	0.666667

Known

FID_2	236	237	238	239	240	241	242	243
known sqrt	1.552264	1.099784	1.843909	1.334523	1.242118	1.45733	1.387015	1.552264
v/n	0.172474	0.122198	0.204879	0.14828	0.138013	0.161926	0.154113	0.172474

FID_2	236	237	238	239	240	241	242	243
known mean	1.133333	1.266667	1.6	1.266667	1.4	1.533333	1.266667	1.866667
(v/n)+(v/n)	0.277043	0.222169	0.33545	0.263035	0.324253	0.353764	0.276311	0.288756
sqrt	0.526349	0.471348	0.57918	0.51287	0.569433	0.59478	0.525653	0.53736
mean-mean	0.333333	0.6	0.266667	0.333333	0.066667	0	0.333333	1.2

FID_2	236	237	238	239	240	241	242	243
classification	0.633294	1.272945	0.460421	0.649938	0.117076	0	0.634132	2.23314

Random

random sqrt	1.302013	1.060099	2.016598	1.496026	1.907379	1.222799	1.302013	1.698739
FID_2	244	245	246	247	248	249	250	251
v/n	0.144668	0.117789	0.224066	0.166225	0.211931	0.135867	0.144668	0.188749

FID_2	244	245	246	247	248	249	250	251
random mean	1.533333	1.133333	1.933333	1.666667	1.933333	0.933333	1.133333	1.8

Known

FID_2	244	245	246	247	248	249	250	251
known sqrt	1.234427	1.759329	1.791514	2.22967	1.496026	1.76743	1.632993	1.407463
v/n	0.137159	0.195481	0.199057	0.247741	0.166225	0.196381	0.181444	0.156385

FID_2	244	245	246	247	248	249	250	251
known mean	1.666667	1.666667	1.933333	1.4	1.666667	1.866667	1.666667	1.133333
(v/n)+(v/n)	0.281827	0.31327	0.423124	0.413966	0.378156	0.332248	0.326112	0.345134
sqrt	0.530873	0.559705	0.650479	0.643402	0.614944	0.576409	0.571062	0.587481
mean-mean	0.133333	0.533333	0	-0.26667	-0.26667	0.933333	0.533333	-0.66667

FID_2	244	245	246	247	248	249	250	251
classification	0.251158	0.952883	0	-0.41446	-0.43364	1.61922	0.933932	-1.13479

Random

random sqrt	1.496026	2.218966	3.150208	6.47486
FID_2	252	253	254	255
v/n	0.166225	0.246552	0.350023	0.719429

FID_2	252	253	254	255
random mean	1.333333	2.066667	2.266667	3.266667

Known

FID_2	252	253	254	255
known sqrt	1.060099	0.96115	0.915475	1.804756
v/n	0.117789	0.106794	0.101719	0.200528

FID_2	252	253	254	255
known mean	1.133333	0.733333	0.533333	0.6
(v/n)+(v/n)	0.284014	0.353346	0.451743	0.919957
sqrt	0.53293	0.594429	0.672118	0.959144
mean-mean	-0.2	-1.33333	-1.73333	-2.66667

FID_2	252	253	254	255
classification	-0.37528	-2.24305	-2.57891	-2.78026

APPENDIX B

1. Articles or papers published in peer-reviewed journals (specify whether in print, accepted for publication, or submitted for publication).

Blom. R. 2005, Imaging Radar Data and Detection of Archaeological Sites. Submitted to *Journal for Conservation and Management of Archaeological Sites (CMAS).*

Comer, D. 2005, History and Status of Aerial and Satellite Remote Sensing and GIS in the Inventory and Evaluation of Cultural Sites. Submitted to *Journal for Conservation and Management of Archaeological Sites (CMAS).*

2. Technical reports (specify whether in print, accepted for publication, or submitted for publication).

Blom, R., and Comer, D., 2002, Detection and Identification of Archaeological Sites and Features Using Synthetic Aperture Radar (SAR) Data Collected from an Airborne Platform, 2002 SERDP Annual Report, report on file, SERDP program office, Arlington, Virginia.

Blom, R., and Comer, D., 2003, Detection and Identification of Archaeological Sites and Features Using Synthetic Aperture Radar (SAR) Data Collected from an Airborne Platform, 2003 SERDP Annual Report, report on file, SERDP program office, Arlington, Virginia.

Blom, R., and Comer, D., 2004, Detection and Identification of Archaeological Sites and Features Using Synthetic Aperture Radar (SAR) Data Collected from an Airborne Platform, 2004 SERDP Annual Report, report on file, SERDP program office, Arlington, Virginia.

3. Conference/Symposium Proceedings and/or Papers scientifically recognized and referenced (other than Abstracts).

Blom, R., 2003, AIRSAR Characteristics. Paper presented at the symposium New Imaging Tools for Archaeological Explorations and Conservation Science: Airborne Synthetic Aperture Radar (AIRSAR) Applications in Central America, Dumbarton Oaks, Washington, D.C.

Blom, R., 2005, Imaging Radar Data and Detection of Archaeological Sites. US/ICAHM Geophysical Technologies in Cultural Resource Preservation Symposium, 8th Annual US/ICOMOS International Symposium, Charleston, South Carolina.

Blom, R., and Comer, D., 2003, Possible AIRSAR Mission To Mesoamerica and South America: Technology and Application to Archaeological Research and Management. Mundo Maya Alliance Conference, Washington, DC.

Blom, R., Comer, D., and Yatsko, A., 2001, locating archaeological sites using AIRSAR derived data. Italy-United States Workshop: The Reconstruction of Archaeological Landscapes Through Digital Technologies, Boston, MA.

Blom, R., Comer, D., and Yatsko, A., 2002, Application of airborne SAR and GIS to San Clemente Island archaeology: GSA Annual Mtg., Denver CO.

Blom, R., D. Comer, B. Byrd, and A. Yatsko, 2001, Locating archaeological sites using AIRSAR derived data. Italy-United States Workshop: The Reconstruction of Archaeological Landscapes Through Digital Technologies, Boston, MA.

Blom, R. Comer, D., Freeman, T., Hensley, S., Moore, E., Yatsko, A., and Zarins, J., 2004, Application of Remote Sensing and GIS to Archaeology: Examples from Diverse Environments. Keynote at International Conference on Remote Sensing Archaeology, Beijing, China.

Comer, D., 2002, Detection and Identification of Archaeological Sites and Features Using Radar Data Acquired From Airborne Platforms. Proceedings for the 2002 AIRSAR Earth Science Applications Workshop. Jet Propulsion Laboratory (JPL), California Institute of Technology, Pasadena, California.

Comer, D., 2003, Archaeology and Preservation Goals of AIRSAR Deployment Central America. New Imaging Tools for Archaeological Explorations and Conservation Science: Airborne Synthetic Aperture Radar (AIRSAR) Applications in Central America. A Round Table at Dumbarton Oaks, Washington, D.C.

Comer, D., 2003, Developing Protocols for the Use of Airborne SAR in Archaeological Inventory. Society for Conservation GIS, 2003 Annual Meeting, Asilomar, California.

Comer, D., 2004, Application of Airborne Radar, Remote Sensing, GIS and Modeling to San Clemente Island Archaeology. The Geological Society of America Annual Meeting, Salt Lake City, UT.

Comer, D., 2004, History and Status of Aerial and Satellite Remote Sensing and GIS in the Inventory and Evaluation of Cultural Sites, presented at SERDP Partners in Environmental Technology Symposium and Workshop.

Comer, D., 2004, Management Zones as Geospatial Tool to Integrate Installation Activities. *Proceedings of the Tenth Forest Service remote sensing applications*

conference. American Society for Photogrammetry and Remote Sensing [CDROM], Salt Lake City, UT.

Comer, D., 2005, History and Status of Aerial and Satellite Remote Sensing and GIS in the Inventory and Evaluation of Cultural Sites. US/ICAHM Geophysical Technologies in Cultural Resource Preservation Symposium, 8th Annual US/ICOMOS International Symposium, Charleston, South Carolina.

Comer, D., 2005, Inventory of Archaeological Sites Using Radar and Multispectral Data. National Geographic Society, Washington, DC.

Comer, D., 2005, Using Radar and Multispectral Data to Inventory Archaeological Sites on San Clemente and Santa Catalina Islands. Cotsen Institute, UCLA, Los Angeles, CA.

Comer, D., Blom, R., Quilter, J., Chapman, B., and Golden, C., 2005, Inventory of Archaeological Sites Using Radar and Multispectral Data. Paper presented at National Geographic Society Roundtable, *Evaluating the Implementation of AIRSAR as an Archaeological Tool in Mexico and Central America*. National Geographic Society Headquarters, Washington, D.C.

Comer, D., et al., 2003, Possible AIRSAR Mission To Central America and South America. AIRSAR Applied to Archaeological Research and Management. NASA Suborbital Workshop.

4. Published Technical Abstracts (e.g., SERDP's Annual Symposium).

Blom, R. and Comer, D., 2002, Detection and Identification of Archaeological Sites and Features Using Synthetic Aperture Radar (SAR) Data Collected from an Airborne Platform Abstract. 2003 SERDP Poster Session PARTNERS IN ENVIRONMENTAL TECHNOLOGY SYMPOSIUM & WORKSHOP.

Blom, R., and Comer, D., 2003, Detection and Identification of Archaeological Sites and Features Using Synthetic Aperture Radar (SAR) Data Collected from an Airborne Platform Abstract. 2003 SERDP Poster Session PARTNERS IN ENVIRONMENTAL TECHNOLOGY SYMPOSIUM & WORKSHOP.

Blom, R., and Comer, D., 2004, Detection and Identification of Archaeological Sites and Features Using Synthetic Aperture Radar (SAR) Data Collected from an Airborne Platform Abstract. Department of Defense Conservation Conference, Savannah, GA

Blom, R., and Comer, D., 2004, Detection and Identification of Archaeological Sites and Features Using Synthetic Aperture Radar (SAR) Data Collected from an Airborne

Platform Abstract. 2003 SERDP Poster Session PARTNERS IN ENVIRONMENTAL TECHNOLOGY SYMPOSIUM & WORKSHOP.

5. Published Text Books or Book Chapters.

Comer, D., and Blom, R. (In press), Detection and Identification of Archaeological Sites and Features Using Synthetic Aperture Radar (SAR) Data Collected From Airborne Platforms. *Remote Sensing in Archaeology*. Springer Press, New York.

APPENDIX C

1. Patents

None

2. Protocols

The protocols developed under SI-1260 have been found to be eligible for use under the Navy's Broad Agency Announcement (BAA) for Innovative Environmental Technologies and Methodologies. Formal notification has not yet been received.

3. EPA/State Regulatory Permits

None

4. Awards

2005
National Center for Technology Transfer and Preservation (NCPTT) grant, *Merging Aerial Synthetic Aperture Radar (SAR) and Satellite Multispectral Data to Inventory Archaeological Sites.*

2005
National Science Foundation (NSF) grant, *Archaeological Application of Airborne Synthetic Aperture Radar Technology in Southern Mexico and Central America.*

5. Scientific/technical honors received

None